NUCLEATION OF SOME TETRACYANOPLATINATE(II) SALTS FROM AQUEOUS SOLUTION

NUCLEATION OF SOME TETRACYANOPLATINATE(II) SALTS FROM AQUEOUS SOLUTION

by

OWUSU AKYIAW BEMPAH M.Sc.

A Thesis

Submitted to the Faculty of Graduate Studies

in Partial Fulfilment of the Requirements

for the Degree

Doctor of Philosophy

McMaster University

May 1972

To

Nana Amoaso

and Papa

DOCTOR OF PHILOSOPHY (1972)
(Chemistry)

McMASTER UNIVERSITY
Hamilton, Ontario

TITLE: Nucleation of Some Tetracyanoplatinate(II) Salts from Aqueous Solution

AUTHOR: Owusu Akyiaw Bempah, M.Sc. (Moscow State University, Moscow)

SUPERVISOR: Dr. O. E. Hileman, Jr.

NUMBER OF PAGES: vii; 86

SCOPE AND CONTENTS:

A brief review of the theoretical and experimental methods applicable in the study of nucleation from aqueous solution is presented. A detailed description of the droplet technique experimental method is given.

Microscopic fluorescence technique has been devised and used successfully for the study of nucleation from aqueous solution of tetracyanoplatinates of barium, calcium and magnesium. This method of detection has been compared with detection of the forming phase by plane polarized light - a well established method.

Evidence has been provided for the mean lifetime of an embryo in aqueous ionic solution and expression for same has been used. The parameters have been compared with those obtained using the Volmer-Becker-Doring classical theory and with published values.

ACKNOWLEDGEMENT

The author wishes to thank Dr. Orville E. Hileman, Jr., for his advice, helpful criticisms and suggestions. The good relationship which developed between us and made working on this project a pleasure - despite moments of frustration - is gratefully appreciated.

Also he wishes to thank Dr. Hoffman for his advice and Raymond Prime for fruitful discussions.

Financial assistance provided by the Province of Ontario and McMaster University is also acknowledged.

Finally, the author joins with the tradition of millions by expressing gratefulness to his wife, Mazie, for her encouragement and coffee - they were both hot!

TABLE OF CONTENTS

LIST OF TABLES

LIST OF FIGURES

CHAPTER 1

INTRODUCTION

1.A. Historical Background

Crystallization is one of the oldest analytical techniques used in Chemistry. It has long been recognised that the process takes place in two stages; namely, the birth of one phase from another, called nucleation, and the subsequent growth of the newly formed phase. The nucleation process is of wide significance in science. Published work relating to it is extremely diverse and interdisciplinary. A few isolated examples are cloud condensation, photography, polymer crystallization, metal solidification, bubble formation and bone formation.

Nucleation is important because in many respects it controls the number, size, structure and morphology of precipitated crystals. The process can occur on its own - homogeneous nucleation - or can be catalysed by foreign agents - heterogeneous nucleation. Historical accounts of nucleation are generally of the latter type; namely, nucleation which has been set off as a result of mechanical agitation, or the addition of crystals of the solute or some foreign particles.

Fahrenheit [1] in 1714, while using his newly invented thermometer in the study of freezing of water, initiated the study of phase equilibria and of the undercooling phenomena. His observations were confirmed and expanded by other workers. By 1775 Lowitz [2] had discovered supersaturation phenomena in aqueous salt solutions and had emphasised the analogy with supercooled water.

In the middle of the nineteenth century Lecoq de Boibaudran [3] found

that spontaneous (homogeneous) nucleation occurred in highly supersaturated solutions and apparently did not occur in solutions of lower supersaturation. Osward [4] distinguished two types of supersaturated solutions, metastable and labile, and showed that homogeneous nucleation is possible only in labile solutions. He demonstrated that for the same solute in the same solvent, the concentrations of metastable solutions are less than those of labile solutions.

Attempts to link undercooling (supersaturation) with the rate of formation of nuclei was first made by Tammann [5]. He observed that the rate of nuclei formation in water was too small to be measured by his method unless the undercooling exceeded 50C°.

At the beginning of this century, Ingersoll and Mendenhall [6] found that droplets of gold, platinum and rhodium, 50-100 μ in diameter, often could be supercooled over 100C° before freezing. At that time it was well known that the bulk liquid could be supercooled only a few degrees. Vonnegut [7] in 1948 explained that bulk nucleation was heterogeneous and that if the bulk was broken up into droplets, some of these droplets would be catalyst-free and therefore could be supercooled by many degrees. Since then many workers [8,9,10] have used the droplet technique in nucleation studies from the melt and from solution.

1.B. Nucleation Theory

1.B.1. Classical Nucleation Theory

Most of the basic theory believed to be applicable to crystal formation from solution or from the melt are extensions of theories originally derived for condensation from the vapour. The theory, due to Volmer and Weber [11], was derived from thermodynamic considerations; that is, it presupposed an equilibrium situation between the various sized clusters.

1.B.1.a. Qualitative Considerations

Qualitatively, the reaction between ions and molecules which lead to cluster formation and eventually to evolution of crystals has been likened to chemical reaction. In the chemical reaction, the activation energy is the energy barrier which must be surmounted before products may be formed, and similarly an energy barrier to nucleation must be overcome before crystallization can occur. One direct result of this energy barrier is the necessary creation of some degree of supersaturation before spontaneous crystallization will occur.

In solutions at normal temperatures the molecules or ions of solute are in constant motion and therefore spend part of the time within the sphere of influence of another molecule or ion. Hence groups of molecules or ions are always present when the solute is present in any, other than trivial, concentration. There is, though, a distinct difference between the behavior of ions and molecules. Because of their ionic charge, ions tend to associate themselves with neutral or oppositely charged groups, while uncharged molecules do not suffer this restriction.

The situation then, prior to nucleation, involves the continuous formation and dissolution of ionic or molecular clusters in equilibrium with all other clusters and monomers. If the concentration of solute ions or molecules is large enough a few clusters become sufficiently large to consolidate themselves into small crystallites whereupon the supposedly irreversible process of crystal growth ensues.

The maximum-sized cluster which may exist before spontaneous crystallization sets in is usually referred to as the critical nucleus. In terms of molecular aggregation the process may be represented, according to

Szilard and Farkas [12], as follows.

$$A_1 + A_1 \rightleftharpoons A_2$$

$$A_2 + A_1 \rightleftharpoons A_3 \qquad (1)$$

$$\vdots \qquad \vdots$$

$$A_{x-1} + A_1 \rightleftharpoons A_x \quad \text{(critical nucleus)} \qquad (2)$$

$$A_x + A_1 \xrightarrow{\text{Nucleation}} A_{x+1} \qquad (3)$$

$$A_{x+1} + A_1 \longrightarrow \text{Crystal growth} \qquad (4)$$

This mechanism involves only elementary kinetic processes; that is, a cluster, A_i, which contains iA molecules may capture or lose an "A" molecule and become an A_{i+1} or A_{i-1} cluster. All other processes, such as the formation of a large cluster by the collision and union of two smaller clusters, or the fission of a large cluster into smaller ones, or the simultaneous aggregation of single molecules, are excluded as being less probable.

By imagining some mechanism which removes crystals above a certain size, dissociates them and then returns the single molecules to the system. a stationary reaction state results. In this state, the numbers of the various species remain constant, and there is a steady flux of crystals through the system. This flux is the steady state nucleation rate.

1.B.1.b. Quantitative Theory

After the concept of Szilard and Farkas became established, their kinetic scheme formed the basis of a number of subsequent analyses of the nucleation problem. The principal paper was that of Becker and Doring [13], although this was based on earlier work of Volmer [14]. The working equation is

$$J = A \exp -\left[\frac{16\pi\sigma^3 v}{3(kT)^3 \ln^2 S}\right] \qquad (5)$$

in terms of the rate of nuclei formation per second per cm^3 for a spherical nucleus. In Equation (5),

v is the molecular volume of the solute;

σ is the surface energy between the crystallite and solution;

S^* is the critical supersaturation ratio; and

kT is a frequency factor.

The pre-exponential factor, A, contains both energy as well as kinetic factors, and is given by the expression

$$A = \frac{NkT}{h} \exp\ [-G_D/kT] \qquad (6)$$

In Equation (6)

N is the number of monomeric units;

$\frac{kT}{h}$ is a frequency factor; and

G_D is the activation energy barrier to diffusion of monomers from the bulk solution to the clusters.

1.B.2. Theory of Induction Times

The time elapsing between the creation of the supersaturated or supercooled state and the appearance of particles by some form of detection device is known as the induction time or "time lag" [15,16,17]. It is expressed in the form

$$t = t_i + t_n + t_g \qquad (7)$$

where:

t_i is the time required to attain the steady state embryo distribution;

t_n is the time required for nucleation; and

t_g is the time required for growth of the nucleus to detectable dimensions.

Attempts at theoretical evaluation of the induction period t have been made by many authors, especially Zeldovitch [18] and Turnbull [19], by making various assumptions and for specific phenomenon. Zeldovitch, for example, calculated the time required for the growth of droplets of appreciable size from nuclei, .e., t_g, with special reference to cavitation; while Turnbull calculated what, presumably, is the sum of t_n and t_i for crystallization from the melt.

Kantrowitz [20] was the first to give a generalised equation by making the assumption that the "time lag" is not affected by the thermodynamic energy barrier and that the decisive factor is the diffusion process by which the system of embryos is formed. One other assumption is that the generation of supersaturation is instantaneous. His rate equation is given by

$$J(t) = J_0[1 + 2\sum_{n=1}^{\infty} (-1)^n \exp\{-n\frac{t}{\tau}\}] \qquad (8)$$

where:

n is the number of molecules in the nucleus;

J_0 and J(t) are the rate of nucleation at t = 0 and t simultaneously; and

τ is a factor which is equated approximately with t_i of Equation (7).

For purposes of homogeneous nucleation none of the factors on the right side of Equation (7) have been evaluated independently until recently. Frisch and Carlier [21] have considered the whole question of induction period or "time lag". Their expression (in their notation) is

$$L = L_1 + X/T \qquad (9)$$

where

L is the induction time or "time lag";

L_1 has been shown by Goodrich [22] to represent the mean life-time of

the critical-sized embryo; and

X/T is a constant whose physical significance is not immediately obvious from their report.

In terms of experimentally observable physical parameters L and L_1 (in seconds) may be expressed as follows.

$$L = \frac{4\pi\sigma M}{(NkT)^{1/2}p_\infty S \ln^2 S} \times \left[a - \frac{a^2}{2(2\pi)^{1/2}} + \frac{a^2 \ln S (kT)^{3/2}}{24\pi v_\beta \sigma^{3/2}}\right] \quad (9)$$

and

$$L_1 = \frac{(\pi)^{1/2}}{2} \frac{kTN^{1/2}d}{\pi^{1/2}M^{1/2}Sp_\infty} \exp\left[-\frac{(4\pi)^{1/2}(3Md)^{2/3}\sigma}{N^{2/3}kT} + \ln S + \frac{16\pi\sigma^3 M^2}{3N^2 d^2 (kT)^3 \ln^2 S}\right] \quad (10)$$

where:

N = Avogadro's number;

σ = surface tension in dynes per cm;

d = density in gm per cc;

M = the gram molecular weight of solute;

S = supersaturation ratio; and

a = a constant which is greater than unit.

L_1 may be equated with t_n in Equation (7), since nucleation time t_n is the time required by A_n^*, i.e., critical-sized embryo, to acquire the extra molecule or ion to become a nucleus. In terms of the phenomenological theory, then L_1 is the time for completion of the reaction

$$An + 1 = A_{n+1} \quad (3)$$

The expressions for L and L_1 are convenient to use in interpreting experimental results. Further the validity of the expressions could be checked by using other means of calculating the parameters which are

calculable by Equations 9 and 10.

The basic theory suffers from several fairly serious approximations. The first of these is that the equation originally formulated using equilibrium thermodynamics, actually refers to a non-equilibrium situation.

Further, there is objection to the thermodynamic treatment of a droplet or a crystallite as a macroscopic phase. Defay [23] contends that this can be done only so long as it is possible to consider a surface element of the droplet or crystallite as the site of exchange of a very large number of molecules between the liquid and the vapour or solution and crystallite. Thermodynamical equilibrium represents the equalization of this exchange in opposite directions. To say that this equilibrium obeys the law of equalization of chemical potentials ($\mu' = \mu$) is, in reality, a statistical statement about a large number of molecules. It is, therefore, clear that to use the model of droplet/crystallite phase in order to describe a grouping of 20 or even 100 molecules or ions is an extrapolation of a mode of thought which is reliably valid only for a considerably larger drop or crystal.

Again the Gibbs free energy of the classical theory does not take into account the free energy change due to (i) the decrease in entropy accompanying the separation of nuclei from the bulk, (ii) the translational degrees of freedom of the embryo and (iii) the change in the rotational free energy of formation. Several attempts have been made to refine and improve the theory and the process has become mathematically very complex. The main weapon of attack has been statistical mechanics. A short review of "the state of the art" is presented below.

1.B.3. Modern Concepts in Nucleation Theory

The classical theory depends upon viewing the supersaturated vapour as a mixture of ideal gas species, each corresponding to a subcritical embryo of a given size. The equilibrium distribution is then computed. Using a detailed material balance, a rate theory is constructed, predicting that the rate of nucleation is proportional to the equilibrium concentration of the critical-sized embryos. From this, parameters such as the critical radius, surface tension, the number of molecules in the critical nucleus, etc., are calculated.

Attempts at improvement in the theory usually begin at the quasi-thermodynamic level, with various statistical ideas being grafted onto what was already a semimicroscopic framework.

Frenkel [24] was probably the first to have noted that the classical theory did not take into consideration energy contribution due to translation and rotation of the drop-like embryo. His resulting expression was, however, incorrect. Several workers [25,26] have since attempted unsuccessfully to evaluate these factors. Kuhrt [26] showed that the Gibbs-Thompson equation

$$\Delta G_V = -\frac{2\sigma}{r^*} \tag{11}$$

should read

$$\Delta G_V = -\frac{2\sigma}{r^*} - \frac{4}{n^*} \tag{12}$$

where ΔG_V is the free energy change per unit volume of stable condensed phase;

r^* is the critical radius; and

n^* is the critical number of molecules in the nucleus.

The term $\frac{4}{n^*}$ in Equation (12) according to Kuhrt arises from translation and rotation of the droplet.

Lothe and Pound [27] believing Kuhrt's calculation to be in error, presented their own theory. The calculated rate of nucleation, with their correction, changed the classical rate of nucleation, by as much as 10^{17}. In other words, it changed the critical supersaturation ratio of water from 4.9 to 2.84. This is not supported by the known experimental facts on vapour condensation.

Lin [28] and Reiss and Katz [29] have shown that the collective translation contribution was not as large as it had appeared in Lothe-Pound treatment. They believe that molecules in a cluster can rotate freely so that the rotational partition functions cancel each other in the equation for the equilibrium cluster concentration.

A presentation by Abraham and Pound [30] departs from the usual formulation because it does not assume ideal gas conditions for supersaturated vapour. Using the grand canonical ensemble model of statistical mechanics, they based their analysis on the vapour as an imperfect gas. They assumed that actual clusters of molecules of various sizes exist and that there is association/dissociation equilibrium between these clusters. They conclude that the chemical potential of the droplet is not the same as that of the bulk at equilibrium. They express the equilibrium chemical potential as:

$$\mu^* = \mu_o + \frac{3kT}{2i} ; \qquad (13)$$

where i is the number of atoms, ions or molecules in the critical nucleus.

With the use of Equation (13) they calculated a rate of nucleation

which was 10^8 greater than the value given by the classical theory. Sutugin [31] believes the basis of this analysis to be erroneous. Meanwhile, the controversy continues!

Another contentious area in the theory is whether or not the surface tension, usually calculated from the expression for the rate of nucleation is valid. Discussion here tends to be touchy, as the Gibbs dividing surface, by definition, is arbitrary. According to Kondo [32] all choices are equivalent, the numerical value of any surface property varies with each choice. Tolman [33] and Kirkwood and Buff [34] derived the following expression for the effect of droplet size on surface tension in the vapour

$$\sigma(r_s) = \frac{\sigma_\infty}{(1 + [2\delta/r_s])} \tag{14}$$

where σ_∞ is the surface tension in a plane surface,

r_s is the radius of the Gibbs surface of tension, and

$+\delta$ is the distance between the two neighbouring dividing surfaces for a given droplet. Parlange [35] showed that the correction does not appreciably affect the results predicted by the classical theory. Benson and Shuttleworth [36] and Sandquist and Oriani [37] have also shown that the use of the bulk surface tension was accurate to within a few percent even for very small clusters.

The classical nucleation theory, by its mode of derivation, states that the Gibbs free energy of formation is largest during the transformation of an embryo to a stable nucleus. Special attention has, therefore, been paid to this "critical" nucleus, its size and shape, usually assumed spherical or regular. By computer simulation Binsbergen [38] has shown that "nucleation as a stochastic process is not determined by the thermo-

dynamic stability of a single configuration but rather governed by the kinetic probabilities of transition of one configuration to another". In otherwords, there is no "critical" nucleus, although we can still talk about "critical" embryos in a critical region of size and configuration.

In conclusion then it should be mentioned that, although recent developments have shown that various contributions to the energy barrier have been ignored in the early treatment, their calculated values do not seem to be in accord with the experimental facts. Again none of the parameters which were included in these developments can be directly or even indirectly evaluated experimentally. The classical theory, however, adequately accounts for bubble nucleation and it is one of the points of this work to show how crystal nucleation may be represented by this type of approach.

1.B.4. Interfacial Energy

Before proceeding to the experimental evidence in support or otherwise of the modified Volmer equation as applied to crystal nucleation, it is worthwhile examining specific differences between the nucleation of drops from vapour and of crystals from solution.

Firstly, for ionic crystals the collision efficiency between ions is limited by the net charge of the cluster. Other direct modifications of the equations accounting for molecular volume and interfacial energy replacing surface tension, must be made. The term interfacial energy (energy required to form the interface) may be preferred to interfacial tension because of the thermodynamic derivation and, although these terms have often been used interchangeably, sufrace tension and surface

energy of a solid cannot be equivalent because of surface strain considerations. Walton [39] and Walton and Whitman [40] have shown by their calculations that, if relaxation effects are not taken into account, then the smallest clusters are of surface energy about 80% or so higher than for the infinite surface (at least for cubic and orthorhombic crystals). They believe that this increase is due to edge and corner effects and also to the long range order of electrostatic forces.

Since the nucleation of ionic crystals will take place in such a manner that the interfacial energy is a minimum, the possibility of a net charge on the nucleating species should not be overlooked.

1.B.5. Agreement with Experiment

To establish that the theory is true, it is necessary to show that the Gibbs-Kelvin equation is valid, and also that the nucleation process involves a critical supersaturation. The interfacial energy calculated from the experiments are reasonable.

There have been many attempts to determine the solubility of small crystals in order to ascertain whether the small crystals show enchanced solubility as predicted by the Gibbs-Kelvin equation. The most convincing demonstration that increased solubility does occur with small particles is that reported by Enushun and Turkevich [41]. Before this report many workers simply assumed the validity of the equation.

One of the features of the classical theory that is particularly important in the study of nucleation is that it predicts a nucleation rate which is very critically dependent upon supersaturation. The rate of nucleation is negligible until a fairly well defined supersaturation (the critical supersaturation). At supersaturations greater than this, the nucleation rate

is rapid and usually the supersaturation will collapse by a combination of nucleation and growth. The critical supersaturation is the most important parameter in Equation (5) since it can be measured directly by experiment. If one assumes a reasonable value for the rate of nucleation, then σ, the interfacial energy can be calculated. Since this study is concerned with nucleation from aqueous solution the discussion is limited to agreement with theory from work in this area.

In studies on nucleation from solution, it is difficult, at least from experimental results, to distinguish between homogeneous and heterogeneous nucleation. Nielson [42], however, observed that at high concentrations, in a direct mixing experiment, a sudden burst of new particles is produced and postulated that this point represents the true critical supersaturation for the onset of homogeneous nucleation. Walton applied this concept to some of the data already available in the literature and some of his own experimental results [43], and obtained interfacial energies [44] for the solid/solution interface which he termed "reasonable". Nielson [45] and Mealor and Townshend [46] have examined homogeneous nucleation of several salts. The latter authors found that the critical supersaturation, defined as

$$S_{crit} = \frac{\text{ion product}}{\text{solubility product}}$$

was a constant, independent of the concentration ratio of anion to cation in the original mixture.

Another factor which has been of interest in nucleation studies is the pre-exponential factor. This factor contains molecular transport information. Nielson obtained a value of 10^{18} - 10^{22} for the kinetic constant - a close

enough value to the theoretical one which is usually computed at 10^{25}. Values obtained from droplet technique (see below) experiments are rather low and Walton [47] believes that this is accounted for by catalysed nucleation.

Further, a plot of log J vs. $(1/\ell nS)^2$ for various supersaturation ratios close to S* might be made. The interfacial energy can be determined from the slope and the kinetic constant A, from the intercept. This linear relationship has been found experimentally and the values obtained for A and σ are reasonable.

Experimental data on induction time is lacking in the literature. Where it is mentioned it is so ill-defined as to make the values reported meaningful. Kharin et al [48] have reported the induction time for sucrose from aqueous solution. They report t_1, the induction time to be 16.1×10^4 secs. and decreasing sharply to 2.3×10^3 secs. at higher supersaturations. The surface energy values obtained are, however, below unity. More data is obviously required in this area.

1.C. Techniques used in Nucleation Studies from Aqueous Solution

A number of techniques have been used in the quantitative study of the kinetics of crystal nucleation from a metastable liquid or solution phase. Some of the important ones used to produce the necessary supersaturation and to detect the rate of nucleation are listed below. The principal experimental difficulty is the preparation of a liquid system which is free of solid impurities which may act as heterogeneous nucleation catalysis. Many methods of removing solid impurities from aqueous solutions have been proposed mainly by those concerned with the preparation of "optically empty" solutions. For optical experiments, all that is required is that the total

number of motes remaining after purification shall be very small; for nucleation experiments, there must not be a single mote that is effective above temperatures to which it is desired to supercool the melt or the supersaturation desired. This requirement raises two principal experimental difficulties in nucleation studies, namely:

(1) the difficulty of removing all active motes (the smallest possibly being of the order of 10^{-7} cm diameter) from both the solvent and solute; and

(2) the need to keep all reagents out of contact with possible contaminants, e.g., the atmosphere, both during the preparation of the solution and during the subsequent nucleation experiment.

The problem was eventually solved by Vonnegut who subdivided a liquid system into a large number of tiny, non-communicating droplets whose number greatly exceeded the number of foreign nuclei. The foreign nuclei were thus sequestered in a few of the droplets and hence reproducible rate measurements could be made. For a very long time, the only technique for producing supersaturation in macroscopic droplets was by gradual cooling. The main drawback with this method was that only the compounds with high solubility could be studied. Recently, Hileman and Velazquez [49] published a method which has avoided this major difficulty. By this method, supersaturation in macroscope droplets is produced by extracting the solvent only into the surrounding medium. This method combines the advantages of the droplet technique with the fact that with suitably chosen media, salts with any degree of solubility in water can be studied. Other methods which have been adopted for the production of supersaturation are:

(1) The direct mixing of soluble salts of the reaction partners, e.g., sodium chloride and silver nitrate to produce silver chloride. This method

has the obvious disadvantages that motes cannot be removed and also considerable deviations from the intended mixture ratio may occur.

(2) The rapid undercooling of a solution to a temperature below the supersaturation temperature. In such experiments it is possible that non-steady-state nucleation will be observed since nucleation may occur well before the embryo distribution reaches the equilibrium value characteristic of the temperature of measurement. It is also unsuitable for studies on sparingly soluble salts.

(3) The production of one of the ions taking part in the nucleation in the presence of a second one by a chemical reaction in the solution, e.g., the production of sulphate ions in the presence of barium or strontium ions by the reaction

$$2S_2O_3^{2-} + S_2O_8^{2-} \longrightarrow 2SO_4^{2-} + S_4O_6^{2-}.$$

This method is popularly called "Precipitation from Homogeneous Solution" or PFHS.

Having given methods for the production of supersaturation it now remains to give a few of the methods used in detection of the onset of nucleation.

1.C.1. Detection Techniques

(a) Visual Observation. For soluble salts with a fairly high temperature coefficient of solubility and a fast growth rate, e.g., ammonium chloride, the onset of crystal nucleation from aqueous solution can be observed visually either with or without the aid of microscope. Such a method is not too successful when applied to sparingly soluble salts with a slow growth rate.

(b) Conduction. Concentration changes at the moment of nucleus formation

can be measured conductometrically. Such measurements have been used to determine the induction time for a nucleus to form in an unstirred, supersaturated potassium chloride solution. The method has also been successfully applied to the investigation of the precipitation of sparingly soluble salts. The possible catalytic action of the immersed electrodes is a complicating factor to be borne in mind when interpreting the results of such experiments.

(c) Light Scattering. The scattering of light by small solid particles suspended in a homogeneous liquid phase has been used to detect the onset of nucleation in the precipitation of barium sulphate and also to measure the rate of nucleation in supersaturated potassium chlorate solution. This technique has the added advantage that it can be applied to both soluble and sparingly soluble salts.

(d) Thermometry. The rise or fall in temperature which occurs when a salt is precipitated from a supersaturated aqueous solution provides a convenient indication of the onset of crystal nucleation. This method has been used to study the crystallization of sodium chloride, sodium nitrate, sodium chlorate and ammonium nitrate.

Statement of the Problem

While a wide variety of techniques in the study of nucleation is necessary, a more sensitive method of detecting the forming phase is even more desirable. The aim of the present inquiry is to develop and evaluate a microscopic fluorescence method for the study of nucleation from aqueous solution.

The forming phase will be detected by the fluorescence it emits on irradiation with an ultraviolet light source. For purposes of comparison, the effect on plane polarized light by the forming phase, an established

method of detection, will also be used for studies on the same salts under identical conditions.

It is also intended to offer experimental evidence for the length of the "mean lifetime" of an embryo in a supersaturated aqueous solution, and it is hoped that the more sensitive fluorescence method will shorten the time between the formation of the nucleus and the moment of detection. This will enable a more accurate measurement of the mean lifetime. Further, the interfacial energy between the new and mother phases, a factor common to both the "lag time" model as well as the classical model will be evaluated and compared.

CHAPTER II

EXPERIMENTAL

One major problem associated with the use of the droplet technique in nucleation studies is the creation of sufficient supersaturation within each droplet to ensure crystallization. The reduction of solubility by gradually cooling the droplets limits the usefulness of the method to the study of highly soluble substance because of the narrow temperature range available, e.g., 100°C to 0°C. The technique of generating one of the reaction partners in solution limits the number of substances which can be studied.

One distinct feature of the droplet contraction technique is that very high supersaturation can be generated in each of a population of droplets by the selective diffusion of the solvent (water) into the silicone oil. Because of this and other general advantages discussed in Section I.C., and also because the method has been successfully used in this laboratory for nucleation studies from aqueous solution, it was decided to employ the droplet contraction technique in these investigations.

The compounds selected for study must meet the following criteria in order to test the purpose of the thesis:

(i) their crystals and not their aqueous solutions must fluoresce upon irradiation with ultraviolet light, and

(ii) their crystals must rotate plane polarized light.

Compounds which meet, at least in the most part, these criteria are the tetracyanoplatinates of barium, calcium and magnesium. These compounds were thus selected for the study.

A droplet technique experiment consists of two parts: (a) the dispersion of a saturated aqueous solution of the compound in a suitable silicone oil, and (b) photomicrographic recording of the crystallization events occurring in the droplets.

II.A. Apparatus

The dispersions were prepared with the aid of a Virtis microhomogeniser (Fisher Scientific Company) and a 7-ml flask which was obtained as an accessory.

The selection of a suitable number of drops within the desired size range was accomplished by centrifugation (International Clinical Centrifuge, Central Scientific Company, Chicago, Illinois). The apparatus was adapted to enable the rotation of Nessler cups.

The Nessler cups (diameter 1.25 inches, height 1 inch) were made from Nessler tubes (Fisher Scientific Company). The inside bottom of the thoroughly clean and dry cup was coated with a thin layer of clear silicone fluid (viscosity 60,000 cts). The cup was stood upside down in an oven at 160°C for about three days to drain off excess fluid. On cooling, the inside wall of the cup was wiped clean of fluid. Precautions were taken to exclude dust particles from the cup both immediately before and after its preparation.

The dispersions were examined with a M15 polarizing microscope or a M41 Photoplan fluorescent microscope (Vickers Instruments Inc., Scarborough, Ontario).

Photographs of selected fields of view were taken with an Autowind 35 mm camera and 135 Exposure Unit (Vickers Instruments Inc.). The film used was Anscochrome Colour Slide Film - 500 ASA [GAF (Canada) Ltd., Mississauga, Ontario]. The photographs were studied with the aid of a Leitz slide projector.

The slides were projected on a screen made by mounting graph paper on cork-board. The millimetre graph paper allowed accurate measurement of droplet diameters. The diameter of each individual droplet was measured on each successive slide until crystallization occurred in it.

II.B. Preparation of the Salts and their Saturated Solutions

The solutions used in both the preliminary investigations and in the final experiments were prepared as follows.

Magnesium tetracyanoplatinate. A saturated solution of barium tetracyanoplatinate(II) (Alfa Inorganics, Inc., Beverly, Mass.) was prepared by dissolving about 4 gm of the salt in 50 ml of deionized water. The solution was warmed to about 60°C, allowed to cool to room temperature and then filtered. A saturated magnesium sulphate solution was added to the filtrate. The thick white precipitate of barium sulphate was separated from the solution by centrifugation and then filtration. The filtrate was evaporated until a large amount of precipitate formed. The crude magnesium tetracyanoplatinate was collected and recrystallized twice. The saturated solutions used in the nucleation studies were prepared by dissolving the purified salt in deionized water.

Calcium tetracyanoplatinate. The preparation of the calcium tetracyanoplatinate was similar in procedure to that used for the magnesium salt except that calcium chromate solution was used to precipitate the barium from solution.

Barium tetracyanoplatinate. The saturated solutions of the barium salt were prepared from the recrystallized commercial stock.

II.C. Procedure

The procedure adopted here is that used previously in this laboratory

by Velazquez [50]. The aim was to prepare a transparent dispersion in silicone oil which, upon 75× magnification would enable the study of several hundred droplets with a diameter range of 10 to 80 microns. The droplets necessarily had to be on the same optical plane, stationary and must not communicate with each other, thus avoiding coalescence. The Nessler cup, prepared as described in Section II.A., enabled the preparation of dispersions which satisfied these conditions.

About two drops (∿0.5 ml) of a freshly filtered saturated solution of the appropriate salt was placed in the microhomogeniser flask containing about 5 ml light mineral oil (viscosity 20 cts). The flask was placed in position on the microhomogeniser stand. The stirrer was lowered to within a few millimeters from the bottom of the flask and the homogeniser turned on for 5 secs at a preselected speed of 4,000 r.p.m. The resulting dispersion was quickly transferred into a centrifuge bottle containing about 5 ml of heavy mineral oil (viscosity 180 cts). The centrifuge bottle and contents were rotated for 60 seconds. By means of a dropping pipette, some of the heavy oil containing droplets of various sizes but no air bubbles was withdrawn and put into the Nessler cup. The Nessler cup was then rotated in the centrifuge for about 90 seconds. Part of the contents of the cup was decanted off, leaving a layer of droplets anchored in silicone fluid. The side of the cup was wiped clean. Silicone oil (viscosity 100 cts) was added and the whole rotated in the centrifuge for about 5 seconds. The mineral oil-silicone oil mixture was decanted off and fresh silicone oil (100 cts) added. This operation was usually repeated two or three times, the aim being the exchange of silicone oil for the mineral oil present. Finally a layer of about 2 mm of silicone oil was left on top the droplet layer. The cup was then placed on the microscope stage, examined, and suitable fields selected.

Photographs of these fields were taken at regular intervals varying from two to four minutes depending on the compound. Exposure time on the polarizing microscope was established automatically by the J35 Exposure Unit, and after preliminary studies four seconds was selected for the fluorescent microscope.

The photographs were developed and the slides, membered in sequence, were projected on the screen. The diameter of each droplet [except the ones of very small initial diameters, ca. 10 microns] was measured on each slide. Also the number of droplets and the time a crystal was first detected in each of them were noted.

CHAPTER III

RESULTS AND DISCUSSION

III.A. Preliminary Results (Qualitative Observations)

One major requirement of the droplet technique experimental system is that the formation of each nucleus must induce the formation of one crystal in one droplet, or in the case of supercooled water, the freezing of the droplet. This implies that the growth rate of the crystallite formed must be fast compared with the nucleation rate so that multiple nucleation in each droplet is avoided. This requirement was met in all the salts described in this study. In the very small droplet with a final diameter range between 8 and 10 microns, the individual droplets solidified completely and suddenly. With the larger droplets, (final diameter range of 20 to 30 microns) however, the crystal(s) formed could usually be detected long before the whole droplet solidified completely. Throughout the experiments a droplet was assumed to have nucleated at the first detection of a crystal.

In the course of observing the droplets under the microscope, droplets were seen to disappear completely and uniformly and then reappear before nucleation occurred. This complete and uniform disappearance of the droplets irrespective of size indicates that there is no concentration gradient from the centre of the droplet to the solution/oil interface. Also, when nucleation occurred, the position of the crystals in the droplets appeared to be random; that is crystals appeared at the edge of some droplets, and in others at the centre. (Of course, there was no way to determine the position of crystals which appeared at the solution/oil interface nearest to, or farthest

from, the microscope objective; they might appear to lie in the centre of the droplet.)

The effect of the reaction medium (silicone oil and silicone grease) was also studied. Table 1 shows the combinations used. The data for $t_{1/2}$ is found for the calcium salt. The $t_{1/2}$ was taken as the time (in laboratory coordinates) when 50% of the droplets under observation had crystals in them. Table 1 shows that reaction medium does not affect the nucleation process. Similar studies made on the other salts gave results which showed that the medium does not affect the rate of appearance of crystals in a droplet.

It has been suspected that in droplet experiments where many droplets in close proximity are observed at the same time, dendrites shoot from crystallized droplets and catalyse the nucleation of neighbouring droplets. This "neighbourhood effect" if present will generate a nucleation "front"; that is, the slides will show a field of droplets in which droplets with crystals in them will appear first from one side of the field and progress to the other. This effect was observed in the preliminary studies on ammonium tetracyanoplatinate. Because of this the salt was rejected from any further study. In the case of the compounds studied, the absence of local extraneous effect on particular droplets was indicated by the fact that the spatial distribution of the order in which crystals appeared in the droplets was found to be entirely random.

The size range studied for all the compounds was 10 through 60 microns final diameter. It was found that droplets which did not nucleate included droplets of all diameter ranges. Therefore the probability of crystals not appearing in a droplet did not depend on its size.

TABLE 1

Effect of reaction medium on droplet nucleation (for calcium salt)

Silicone Oil	Silicone Grease	$t_{1/2}$ (min)
100 cts (used as purchased)	1 million cts	43
100 cts	60,000 cts	56
100 cts (vacuum dried)	1 million cts	56
	60,000 cts	47
200 cts (used as purchased)	1 million cts	61
200 cts (used as purchased)	60,000 cts	45

Mean $\bar{t}_{1/2}$ = 51.3 min.

σ_{SD} = 7.6

Statistical consistency of the data was also considered; since data from four or five sets of experiments, conducted over a period of time, were necessary to enable a significant number of droplets to be obtained for analysis. The $t_{63\%}$ test was used to find whether there were any significant differences between experiments on the same salt under nearly identical conditions. This test (explained later in Section III.B.) showed that the reproducibility of the experiments was satisfactory because $t_{63\%}$ was about the same for a particular salt. But $t_{63\%}$ was considerably different from other compounds, even though the reaction medium and the droplet size-range were about the same. (For the preliminary experiments only about 50 droplets were analysed from each experiment.) As a result of these observations, all the droplets which were obtained in the final experiments for a particular salt were analysed together, irrespective of the time separating different experimental runs.

III.B. Data Analysis

The initial growth rate of a crystal nucleus is known to be slow and is nucleation controlled. The hypothetical variation of the radius of a compact nucleus growing from the melt with time, first postulated by Jacobs and Tomkins [51], is illustrated in Fig. 1. The actual function r(t) is represented by the smooth curve ABC. The nucleus is formed and commences to grow at A. Growth after B is rapid and diffusion controlled. Neilsen's [52] induction time for nucleation and diffusion controlled growth of the nucleus in solution, of the order of microseconds, probably refers to the time interval between B and D.

A crystal nucleus, composed of ions crystallizing from solution, would be expected to have a slower growth rate compared with growth from the melt for the following reasons:

(a) There is a possibility that the nucleus may be charged. The concentration of charge on a small crystallite is likely to induce an electrical double layer in the immediate area surrounding it. This is likely to slow down addition of monomers.

(b) In solution, it may be necessary, at least in part, to remove the water of solvation of the monomers before addition of ions to the crystallite. It would be expected that the blocking tendency of escaping solvent molecules will prevent rapid growth of the nucleus.

The effect of seeking a more sensitive method of detection in nucleation, then, is to detect the crystal before the point B is reached. A detection method which will reduce t (Fig. 1) or eliminate it altogether will make it possible to measure experimentally the mean lifetime of an embryo more accurately.

So far the only theoretical analysis and a quantitative expression for the mean lifetime of an embryo available is that given by Frisch and Carlier (Equation 10). This expression is used in our analysis because it will enable reasonable comparison to be made between L_1 obtained using both the microscopic fluorescene method and the plane polarized light method. The form of the relationship between the logarithm of the mean lifetime of an embryo and the inverse of the square of the logarithm of supersaturation ratio, predicted by their model, is a further check on the assumption made in our analysis.

Further, the method of calculating nucleation rates as well as their dependence on supersaturation from the experimental data is described.

III.B.1. Identification of L_m

It was mentioned in Section II.C. that the diameter of each droplet was measured on each successive slide. This enabled the calculation of the rate of change of droplet diameter to be made, since the slides were taken in a well-defined time sequence in all the experiments. It was found that the

Fig. 1. Hypothetical rate of growth of nucleus with time.

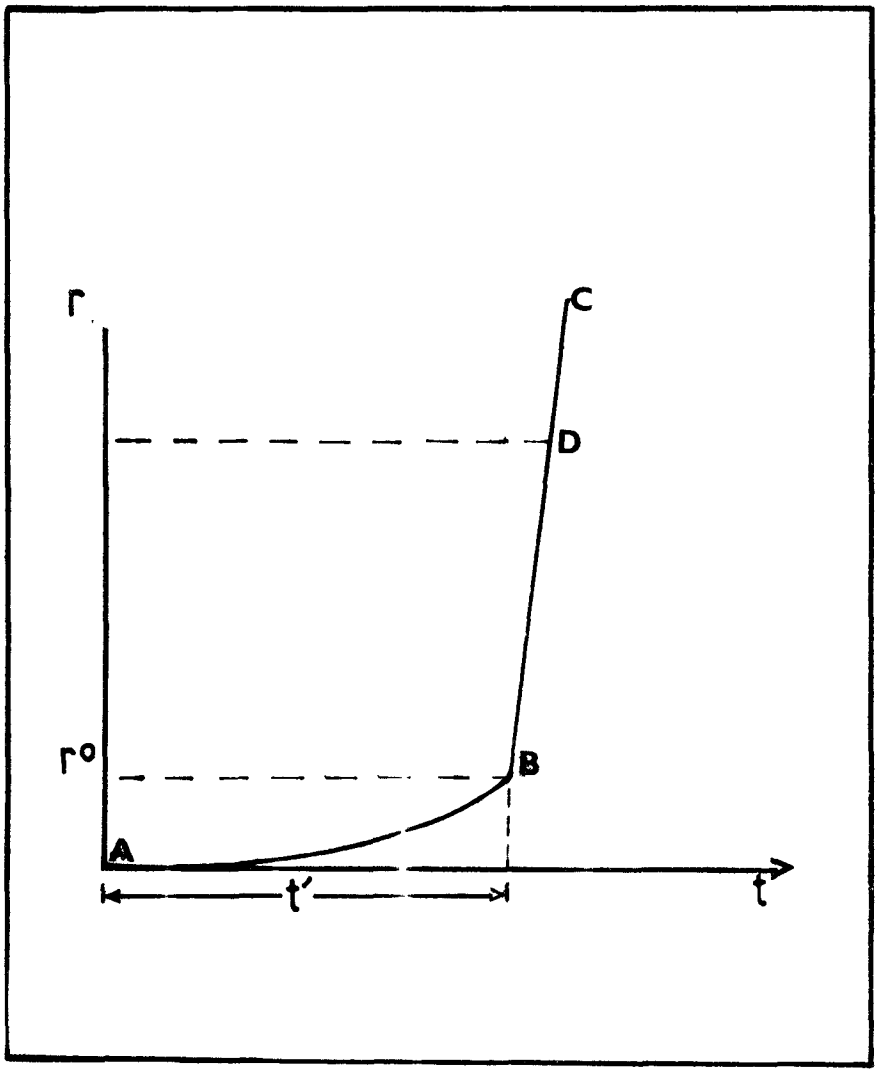
r
C
D
r°
B
A
t'
t

diameter of each droplet decreased sharply and rapidly at the beginning of the experiment but the decrease tailed off until eventually the diameter remained nearly constant for a time before a crystal appeared in the droplet. It was observed that for some droplets, this near constancy of the diameter was not attained before nucleation occurred, but these were very few in number. The time taken by each droplet to reach this near constant diameter range was found to depend on the initial diameter and on its position in relation to other droplets in the field of view.

The picture that emerges for the rate of change of droplet diameter with time is as illustrated in Figure 2. Only curves of two droplets which have the same initial diameter are used for clarity of explanation, even though all the droplets used in this study were similarly analysed. It must be borne in mind that droplets with different initial diameters could, and did have, the same final diameter. Similarly, droplets of the same initial diameter did not necessarily attain the same final diameter.

In Fig. 2, X = 0 is zero time in laboratory coordinates, and represents the time when the first slide picture was taken. $X = t_{BO}$ and t_{AO} is the time in laboratory coordinates at which each droplet diameter was just distinguishable from its final diameter. For most droplets the points "M" and "N" represent about 105% of the final diameter, but for droplets of small final diameter (less than 10 microns) they represent about 110% of the final diameter. $X = t_{BF}$ and $X = t_{AF}$ are the times in laboratory coordinates when a crystal was detected in droplets B and A respectively.

The time intervals L_B and L_A are defined as

$$L_B = t_{BF} - t_{BO} \tag{14}$$

$$L_A = t_{AF} - t_{AO} \tag{15}$$

Fig. 2. Rate of change of diameter of droplet with time.

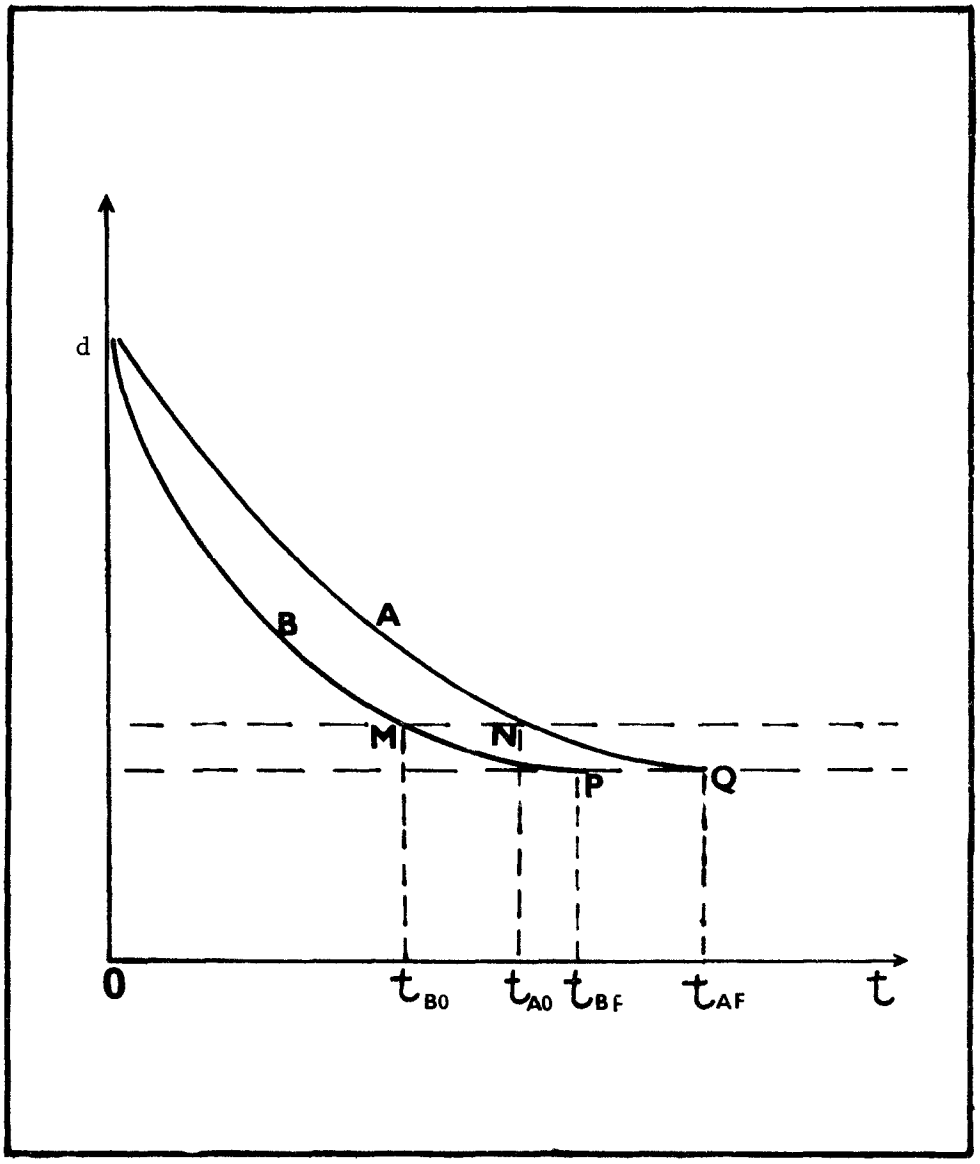
d
A
B
M
N
P
Q
0
t_{B0}
t_{A0}
t_{BF}
t_{AF}
t

The time intervals, as defined above, were determined for all the droplets. For generality, L_A, L_B, etc., will be replaced by L_n, where L_n represents the time interval for the n^{th} droplet. Experimentally, L_n varies from zero to infinity. $L_n = 0$ represents those droplets in which crystals appeared before reaching near constancy in diameter, while $L_n = \infty$ represents droplets in which crystals did not appear at all during the duration of the experiment. Observation was normally stopped when more than 98% of the droplets had crystals in them.

This interval, L_n, was identified with the mean lifetime of an embryo in each droplet. In view of the above, it contains some factor of the growth time t_1 (ref. Fig. 1), but this does not invalidate our analysis, since part of the aim of the analysis is to separate the growth time from the mean life-time. Individual values of L_n are meaningful only when they are viewed as a mean of an aggregate, since nucleation is a probabilistic phenomenon.

Nucleation has long been recognised as a stochastic process. It has been observed that freezing temperatures of a collection of microscopically identical drops of water are spread over a range of several degrees. Similar observation has been made on the solidification of molten metal droplets. Also it has been observed that if these droplets were cooled suddenly to a constant temperature, below their freezing temperature, all the droplets did not crystallize or solidify at once. Phase transformation was spread over a wide interval of time.

These observations have been interpreted on the basis of probability [53,54,55]. In this view, supercooled water or molten metal droplets are

---

In this work further mention of time would be understood as defined by Equations (14) and (15), unless otherwise stated.

like the nuclei of a radioactive substance, a nucleation event in a drop corresponding to the decay of an atom, except that the decay constant is a function of the temperature or degree of supersaturation of the sample. This analysis assumes that all embryos have an equal chance of reaching the critical size by random fluctuations only. The probability (P) of droplets nucleating is experimentally determined by the number of crystallization events (N) occurring in a sample (N_o) in a time interval Δt.

Therefore, in order to obtain a value for L_n which is the mean of an aggregate, all the droplets were grouped according to final diameter. The probability of nucleation with time was plotted on a probability paper. Figure 3a through 3f shows sample data for magnesium tetracyanoplatinate(II). It was found that the time for 63% of the droplets to nucleate, in every size range, was independent of volume. $t_{63\%}$ was similar for all the groups. The choice of $t_{63\%}$ follows from a consideration of Equation 11g in Appendix I.

Briefly, the rate of nucleation J represents the number of nuclei formed per second in unit volume. Thus in a droplet of volume V there are VJdt nuclei formed in time dt. If, during an experiment on droplets, (t_o) is the instant when supersaturation is achieved, and if it is supposed that nucleation takes place as soon as a nuclei is formed, it can be predicted that the instant of nucleation will be given by

$$\int_{t_o}^{t} VJdt = 1$$

and Equation 11g can be written as

$$\ln(1 - P) = -1$$

solving

$$P = 1 - e^{-1}$$

$$= .63.$$

$t_{63\%}$ then is the time when 63% of the droplets would nucleate.

The droplets were then grouped according to supersaturation ratios independent of size, and a histogram of the number of droplets nucleating with time was made. The histograms are shown in Figures 4, 4a, 8 and 10. The median time L_m for the aggregate of droplets at a particular supersaturation was read from the histogram. This was identified with the "mean lifetime" of an embryo at any given supersaturation.

III.B.2. Calculation of Experimental Rate of Nucleation

The method used here is analogous to that used in reducing experimental observations in freezing water drops to nucleation rates. In experiments on supercooled water droplets it can be shown (see Appendix I) that, at constant temperature, if only N of original N_o droplets, each having the same volume V, remain unfrozen after a time interval Δt, then the nucleation rate can be calculated as:

$$J = \frac{1}{V} \cdot \frac{1}{1-P} \cdot \frac{\Delta P}{\Delta t} \qquad (16)$$

where J is the rate of nucleation per second per unit volume (cc) and P is the probability of nucleation.

Although the experiments were not conducted at constant temperature, this parameter is not critical in our studies. The other parameters in the equation are considered below and possible objections to applying Equation 16 to our analysis examined.

The droplet volumes used in this work are not all equivalent as is presumed by the equation; the error involved, however, by using a mean volume is not considerable, especially since the total numbers of the very small and very large droplets in any group of data are less than 10 per cent of the total number of droplets. Since we are dealing with the aggregate of large numbers, this slight deviation is tolerable.

Fig. 4. Histogram of number of droplets nucleating with time for Barium tetracyano platinate. Method of detection: fluorescence technique.

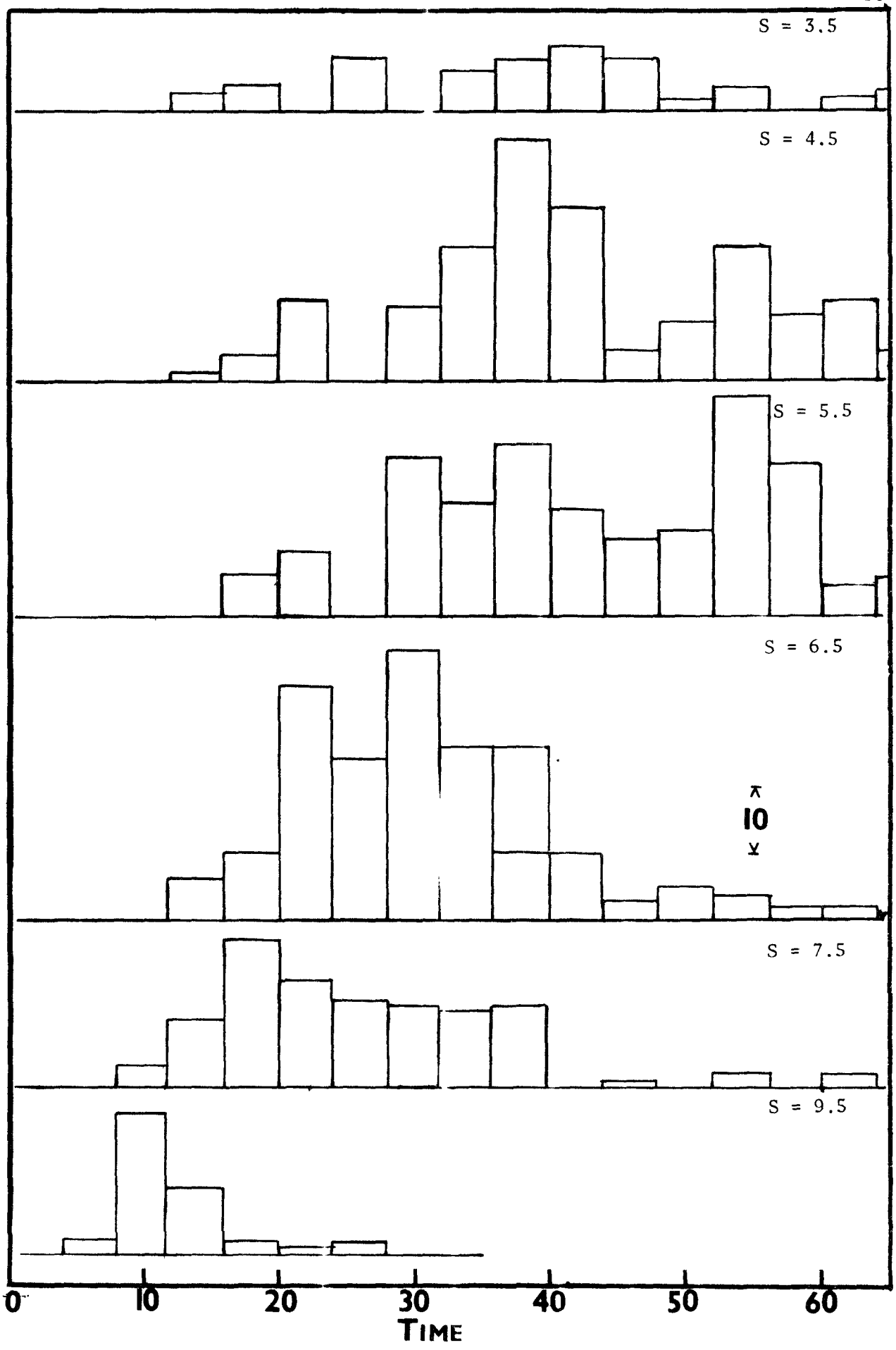
S = 3.5
S = 4.5
S = 5.5
S = 6.5
10
S = 7.5
S = 9.5
0
10
20
30
40
50
60
TIME

Fig. 4a. Histogram of number of droplets nucleating with time for Barium tetracyano platinate. Method of detection: plane polarized light.

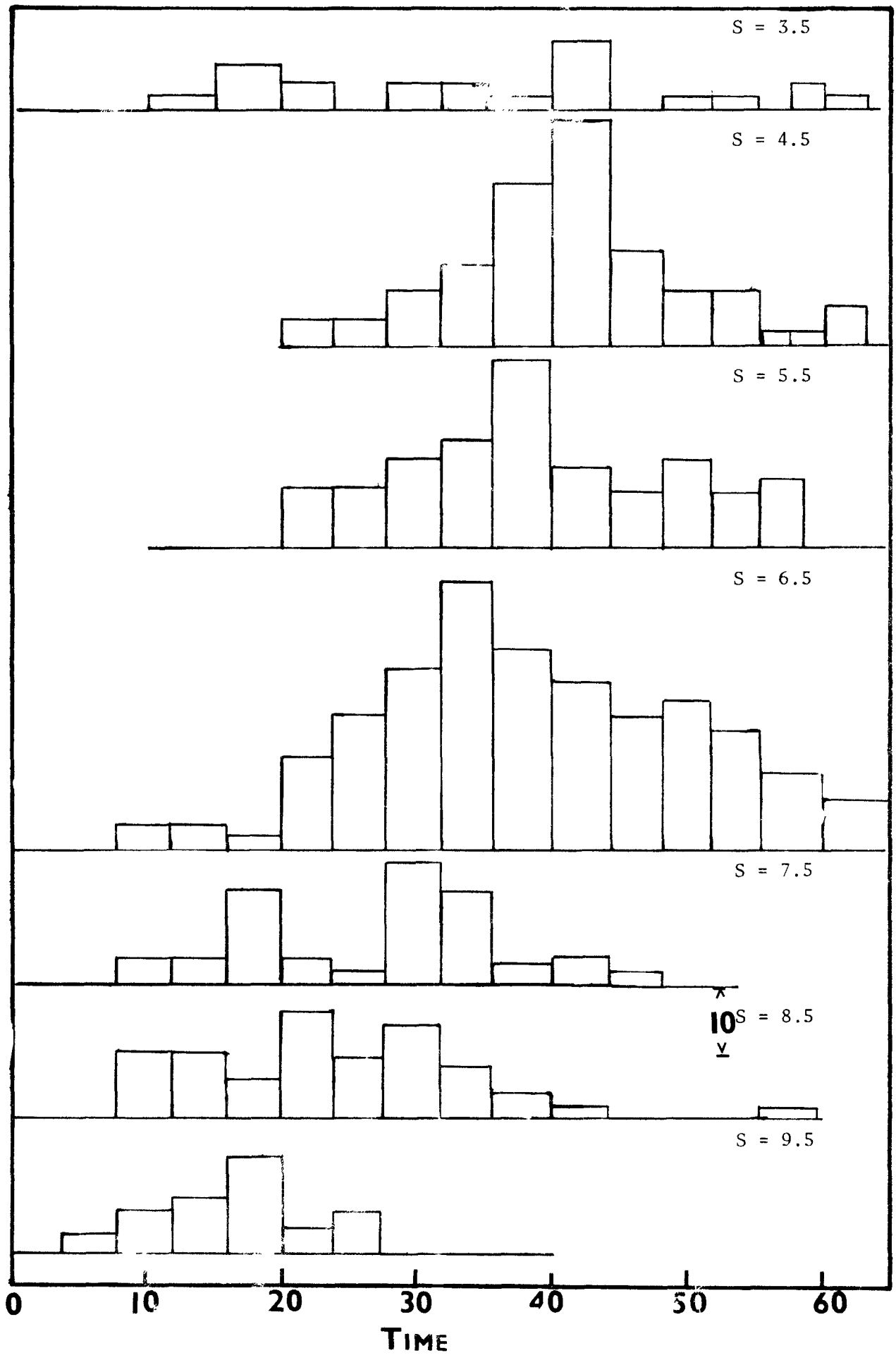
S = 3.5
S = 4.5
S = 5.5
S = 6.5
S = 7.5
10
S = 8.5
S = 9.5
0
10
20
30
40
50
60
TIME

The probabilistic nature of crystal formation in droplets, which is the basis of Equation 16 must also be considered. The probability of a droplet nucleating is determined experimentally by the number of nucleation events (N) occurring in a sample of size (N_o). To make the observed ratio represent reality, a large number of droplets have to be examined. In this work an average of about 900 droplets were examined for each set of data, thus making it feasible to use the equation for our analysis.

Another assumption that is not strictly realizable experimentally is that of constant supersaturation. In view of the expected exponential dependence of the nucleation rate on supersaturation ratio, this too could lead to a serious error in the calculated rate. The error here may be minimised because an average of a large number of droplets has been used.

III.B.3. Calculation of Supersaturation Ratio for Each Droplet

The problem is to find the concentration of any component in a droplet located in a medium in which the solvent is transferring from the droplet to the surrounding medium. Physical transfer is assumed, that is, no chemical reaction at the droplet/bulk phase interface, and transfer corresponds to transfer from a spherical droplet into a stagnant medium. The assumptions in the analysis are that:

(1) The concentration of the transferring component in the bulk phase remains constant during the time interval (i.e., small amounts of transferring phase actually transferred).

(2) The concentration at the droplet/bulk phase interface corresponds to equilibrium conditions.

(3) The droplet has a uniform concentration.

(4) The equilibrium concentration for the transferring component is

independent of the concentration of the non-transferring component in the droplet (this is expected to be realistic for low concentrations). At high concentration, small concentration changes are expected.

Using kinetic considerations (see Appendix II) it has been shown that at the end of time t in laboratory coordinates, from the moment when the dispersion was prepared for observation, the concentration of the solute is given by

$$C_A = (C_{AO}D_0^3)/(D_0^2 - k_2t)^{3/2} \quad (17)$$

where D_0 is the initial diameter;

C_{AO} is the initial concentration of solute in the droplet; and

$(D_0^2 - k_2t)^{3/2}$ corresponds to the final volume of the droplet.

From Equation 17 the supersaturation ratio is calculated as:

$$S = C_A/C_{AO} = D_0^3/(D_0^2 - k_2t)^{3/2} \quad (18)$$

C_{AO} is the bulk equilibrium concentration of solute. In practice, however, S is computed as the cube of the ratio of initial to final diameter.

III.B.4. Calculation of Various Parameters

Because a number of steps were involved either in identifying or defining parameters, it seems necessary to summarise the flow of the calculations here.

From the histogram of number nucleated with time, L_m, taken as the time when the largest number of droplets nucleated, was identified as the mean life-time of an embryo at that supersaturation.

Rewriting Equation 10 in logarithmic form, and writing L_m for L_1

$$\ln L_m = \ln A - B + (16\pi\sigma^3\nu^2)/3(kt)^3\ln^2 S \quad (10a)$$

where A and also B, if σ is assumed constant, are constants. A plot of $\ln L_m$ vs $(\ln S)^{-2}$ was made for each salt studied. The value of σ, the interfacial energy, was calculated from the slope of these curves.

By means of the histogram of number nucleated vs time for each supersaturation ratio, it was possible to obtain the number N of the total N_o nucleating at any time L_m. This gave the probability P of nucleation vs time. The curve of P vs time was drawn on probability paper. The rates of nucleation J were calculated with the aid of Equation 16. An average volume of the droplet population was used for V. P was taken as 50% and the intervals for ΔP as $30\% < P < 70\%$.

The logarithmic form of Equation 5 is

$$\text{Log } J = \log A - (16\pi\sigma^3\nu^2)/3(2.3kT)^3(\log S)^2 \qquad (5a)$$

Using 5a, the series of J values obtained was plotted against their corresponding supersaturation ratios, as log J vs $(\log S)^{-2}$ for each set of data. The values of log A and σ were obtained by intercept and slope respectively.

Other parameters (n*, r*) derivable from the classical Equation 5 were calculated using the values of σ obtained.

The parameter n* is the critical number of particles (ions, molecules, etc.) in a nucleus with a radius, assumed spherical, r*. n* and r* are given by Equations 17 and 18, respectively.

$$n^* = 32\pi\sigma^3\nu^2/3(kT\ln S)^3 \qquad (17)$$

$$r^* = 2\sigma\nu/kT\ln S \qquad (18)$$

All the parameters are shown in Table 5.

III.C. Detailed Discussions and Analysis of Individual Compounds

III.C.1. Barium Tetracyanoplatinate(II)

III.C.1.a. Results obtained with the fluorescene detection method

Table 2 shows the total number of droplets analysed and the subdivisions into supersaturation ratio ranges. If the total number of droplets in each

TABLE 2

Data From the Barium Studies Using F uorescence as Method of Detection

Total number of droplets in subdivisions	Number with crystals	S	$(\log S)^{-2}$	Lm(T) sec.	J $cm^{-3}sec^{-1}$	$\Delta p/\Delta t$
21*		<2.5				
30*	18	2.5±.5				
66	63	3.5±.5	3.38	2400	1.2×10^{6}	2.6×10^{-4}
208	199	4.5±.5	2.34	2160	1.2×10^{6}	2.6×10^{-4}
213	211	5.5±.5	1.82	3120	2.0×10^{6}	4.3×10^{-4}
197	197	6.5±.5	1.51	1680	1.6×10^{6}	3.5×10^{-4}
102	102	7.5±.5	1.31	960	3.7×10^{6}	8.0×10^{-4}
38	38	9.5±.5	1.05	480	8.8×10^{6}	1.9×10^{-3}
29*	29	>10				

*Group of crystals not analysed. Total number of droplets studied was 874.

Mean radius 15 microns.

range was less than 30 droplets, the number was assumed to be statistically not large enough and therefore not analysed.

The probability P of nucleation with time (Fig. 5) for each supersaturation shows that, at low supersaturation ratios, $S \leq 6.5$, two separated populations whose relative frequency distribution curves share a common area are being observed. It is believed that the lower portions of these curves represent heterogeneous nucleation because of the steeper gradient. The upper portion represents homogeneous nucleation.

This may be supported by the fact that, in the absence of foreign surfaces, nucleation of the crystal phase may occur only by the chance orientation of localised groups of ions into a crystal-like configuration. A suitable solid (nucleation catalyst), however, may cause the ions to become locked into the crystal lattice under the influence of its surface force or lack of it. Such an ion or group of ions will not only be bound to the surface of the particle but will have only one exposed surface; on both counts it will be less vulnerable to thermal bombardment than will a spontaneously formed aggregate. Such an embryo will, therefore, have a high probability of attaining the critical size at which it may nucleate the droplet even at low supersaturation.

On the other hand a droplet without a nucleation catalyst at the same supersaturation will contain a relatively few equilibrium numbers of embryos. The embryos will be vulnerable to thermal bombardment and will therefore have a low probability of producing critical embryos which will grow into a detectable crystal in the droplet. Consequently while the two processes are occurring simultaneously in neighbouring droplets the heterogeneous process with higher probability of production of critical embryos predominates at low

Fig. 5. Probability of nucleation of droplet with time. Method of detection: fluorescence.

Legend:

S = 9.5 ± 1.0

S = 7.5 ± 0.5

S = 6.5 ± 0.5

S = 5.5 ± 0.5

S = 4.5 ± 0.5

S = 3.5 ± 0.5

Note: Some points in the probability vs time curves were not used because the number of droplets involved were small.

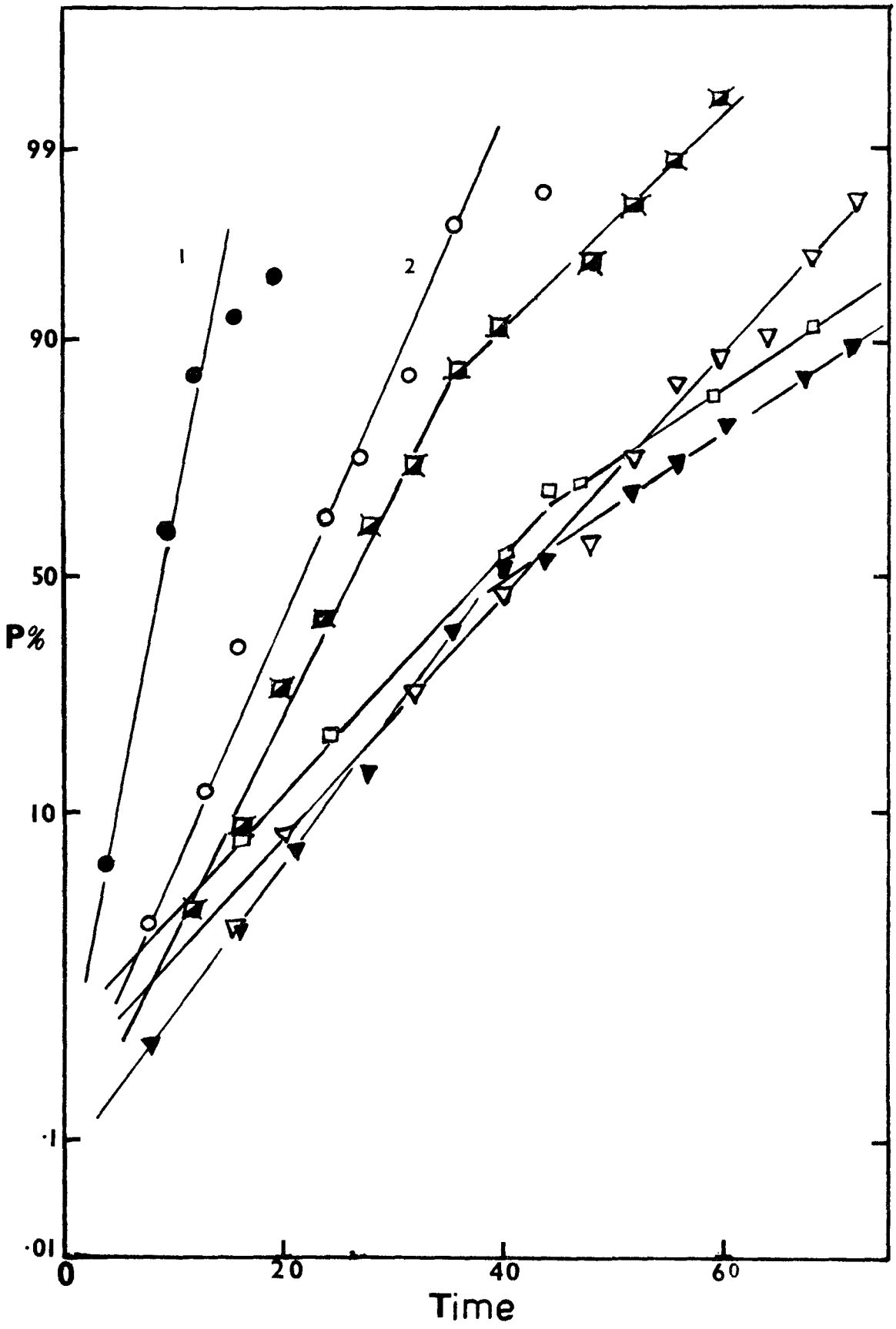
99
90
50
P%
10
·1
·01
0
20
40
60
Time
1
2

Fig. 5a. Probability of droplet nucleation with time. Method of detection: plane polarized light.

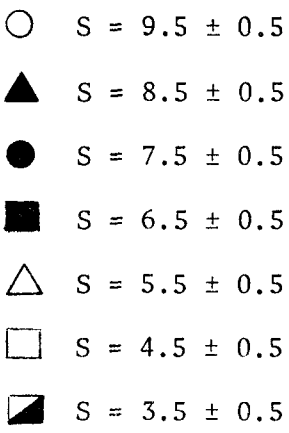

Note: Some points in the probability vs time curves were not used because the number of droplets involved were small.

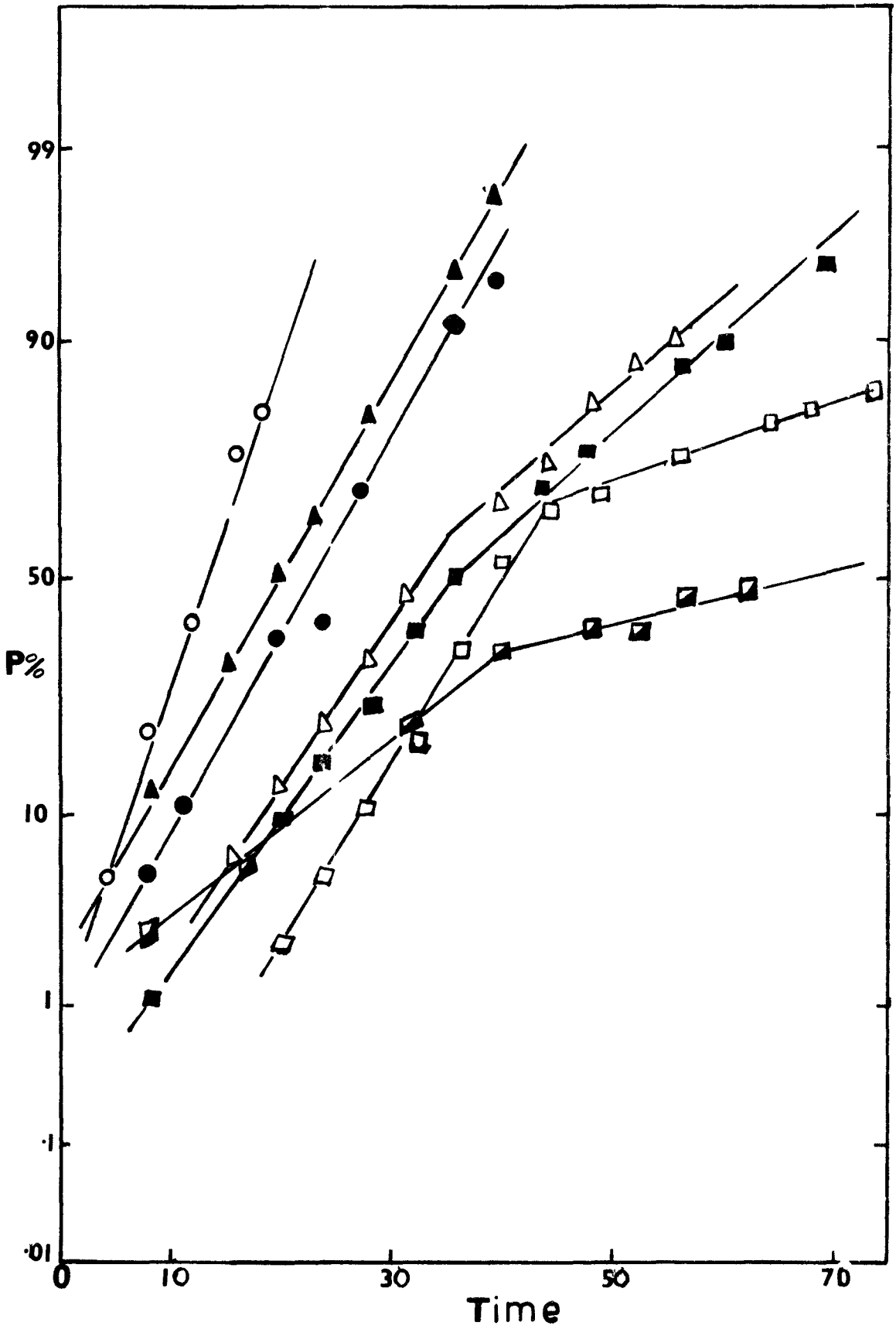
99
90
50
P%
10
1
·1
·01
0
10
30
50
70
Time

supersaturations.

Curves 1 and 2 of Figure 5 represent purely homogeneous nucleation. At such high supersaturations the droplets with heteronuclei are exhausted. The relatively high equilibrium concentration of embryos will have a high probability of producing a critical embryo which will grow to detectable size.

It is believed that the droplets which nucleated at low supersaturation might have contained a number of hetero-nucleated crystals.

These conclusions are confirmed by the position of the median L_m in Fig. 4. L_m increases with increasing supersaturation till S = 5.5 and then begins to decrease with still increasing supersaturation. If it is assumed that hetero-nucleated and homo-nucleated crystallite will require the same time to grow to detectable size by diffusion-controlled growth in solutions of similar supersaturation, then the maximum value exhibited by L_m with increasing supersaturation can only be explained by the simultaneous occurrence of the two processes.

The low value at low supersaturations can be explained by the high probability of heteronucleation because Equation 10 predicts that, for homogenous nucleation, the mean lifetime of an embryo is longest at low supersaturation ($L_m = \infty$ at S = 1) and decreases sharply at very high supersaturations. Therefore if only homogeneous nucleation were being observed L_m will be long at low supersaturations. The maximum appears because L_m, being only an average value, is heavily weighted by the predominance of heterogeneous nucleation with its corresponding short mean embryo lifetime at low supersaturations.

The spread of nucleation events along the time-axis in Fig. 4 is also

TABLE 3

Data from the studies of barium salt using plane polarized light as detection method.

Total number of droplets in subdivisions	Number with crystals	S	$(\log S)^{-2}$	Lm(T) sec	J $cm^{-3}sec^{-1}$	$\Delta p/\Delta t$
36*		<2.5				
17*	7	2.5±.5				
74	57	3.5±.5	3.38	2400	6.4×10^5	1.4×10^{-4}
142	124	4.5±.5	2.34	2400	6.4×10^5	1.4×10^{-4}
157	148	5.5±.5	1.82	2160	1.5×10^6	3.3×10^{-4}
288	280	6.5±.5	1.51	1920	1.6×10^6	3.5×10^{-4}
73	73	7.5±.5	1.31	1480	3.1×10^6	6.7×10^{-4}
82	82	8.5±.5	1.16	960	3.1×10^6	6.7×10^{-4}
40	40	9.5±.5	1.05	960	5.1×10^6	1.1×10^{-3}
20*	20	>10				

*Group of droplets not analysed.

Total number of droplets studied was 929. Mean radius 15 microns.

Fig. 6. Plot of log J vs $1/\log^2 S$ for barium salt. Method of detection: fluorescence.

Note: Some of these points corresponding to low supersaturation (or heterogeneous nucleation) were not used in these curves. For rationale see pages 42-49.

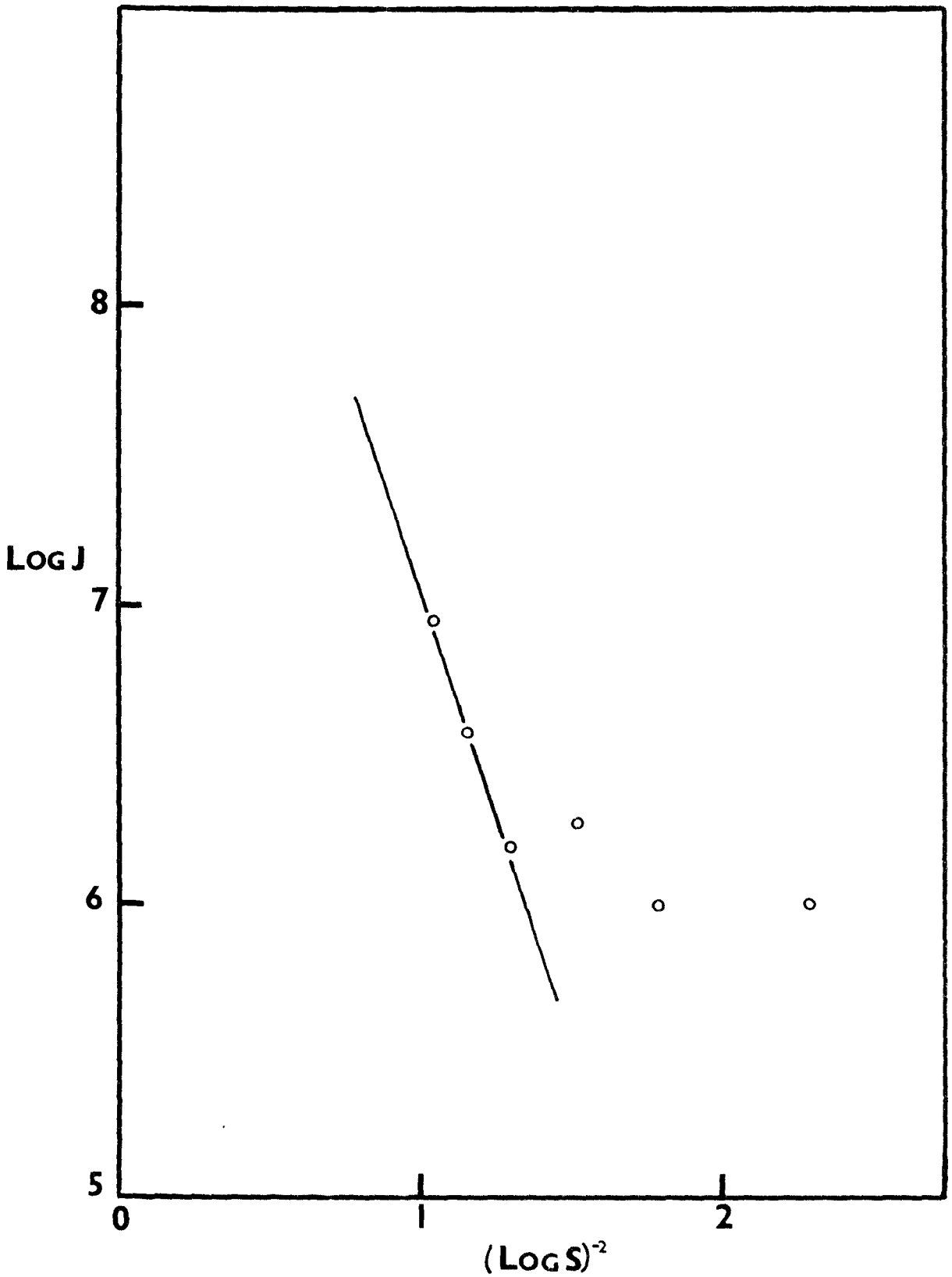
8
7
6
5
LOG J
0
1
2
(LOG S)$^{-2}$

Fig. 6a. Plot of log J vs $1/\log^2 S$ for barium salt. Method of detection: plane polarized light.

Note: Some of these points corresponding to low supersaturation (or heterogeneous nucleation) were not used in these curves. For rationale see pages 42-49.

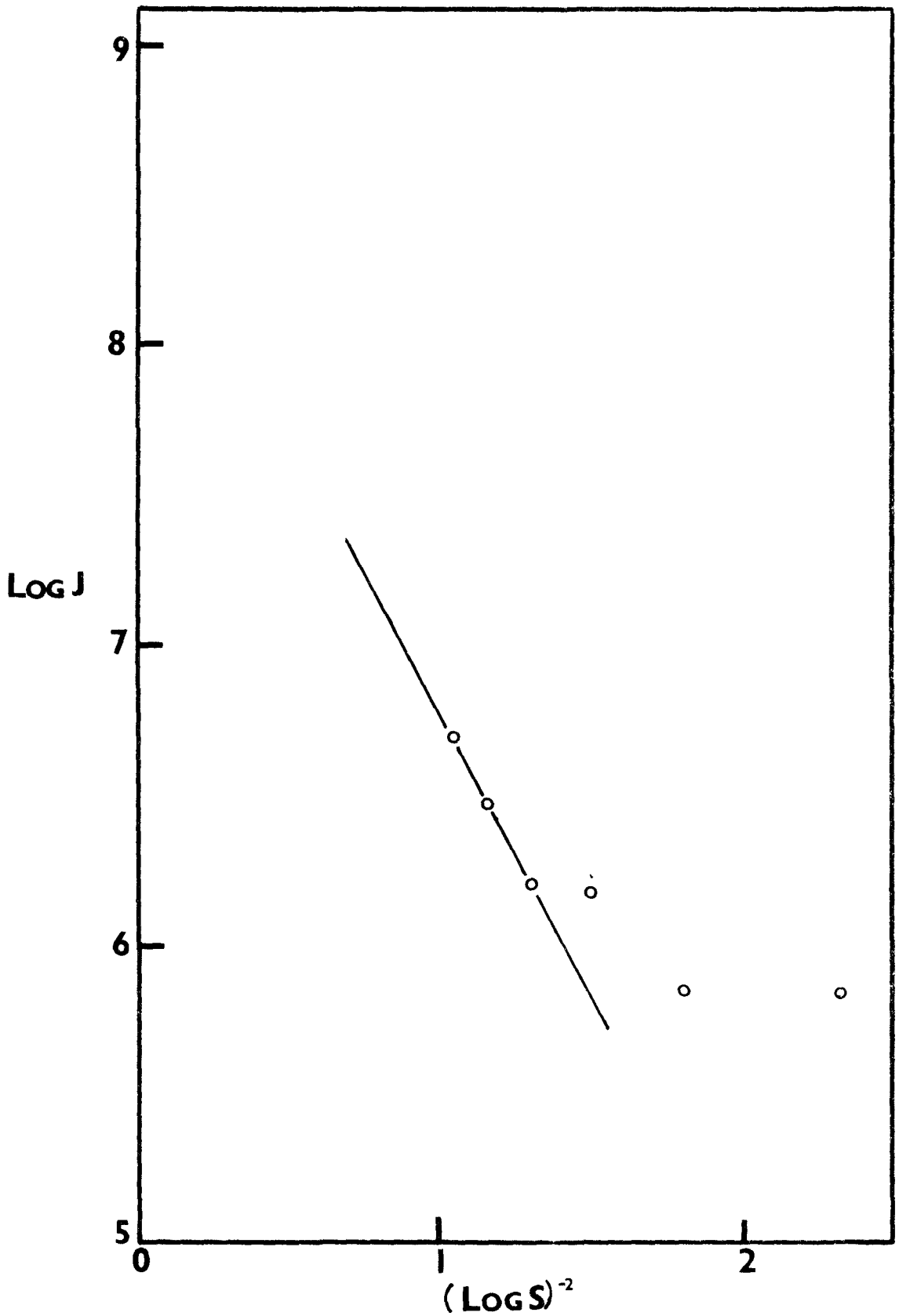
9
8
7
6
5
LOG J
0
1
2
(LOG S)$^{-2}$

significant. A significant number of droplets simply did not nucleate at low supersaturation confirming that some of those droplets without nucleation-catalyst would have long mean lifetime for the embryo. At high supersaturations, however, the horizontal spread is curtailed. We believe homogeneous nucleation is becoming predominant as supersaturation increases. At $S \geqslant 6.5$ all the droplets had crystals in them and the value of L_m also decreases.

The above conclusions that both homogeneous and heterogeneous nucleations are being observed and that low L_m values at high supersaturations correspond to homogeneous nucleation are borne out by Fig. 6 and Fig. 7. Equations 5 and 6 from which these curves were derived are based on two different parameters. They predict a linear relationship between logJ and $(\log S)^{-2}$ and $\log L_m$ and $(\log S)^{-2}$ for homogeneous nucleation. The linear relationship as found in this analysis is true only at high supersaturations.

III.C.1.b. Results obtained with plane polarized light

Table 3 shows the total number of droplets and the subdivisions into supersaturation ratio ranges. The analysis, results and conclusions are similar to those obtained with the fluorescene detection method. Figures 4a through 7a show the corresponding curves. There is one important feature to note in Fig. 4a. The number of droplets that remained without crystals in this set of data is relatively greater when compared with the data from the fluorescene experiment. Further the values of L_m in these experiments are larger than those measured in the fluorescene experiment. These observations can be explained as follows and by referring to Fig. 1. A droplet, containing a crystallite of radius r_o will not require sensitive detection device since growth from B to D requires a time of the order of microseconds, if Nielsen's assessment is correct. It seems to us that the rapid growth portion of the

Fig. 7a. Plot of log T vs $1/\log^2 S$ for barium salt. Method of detection: plane polarized light.

Note: Some of these points corresponding to low supersaturation (or heterogeneous nucleation) were not used in these curves. For rationale see pages 42-49.

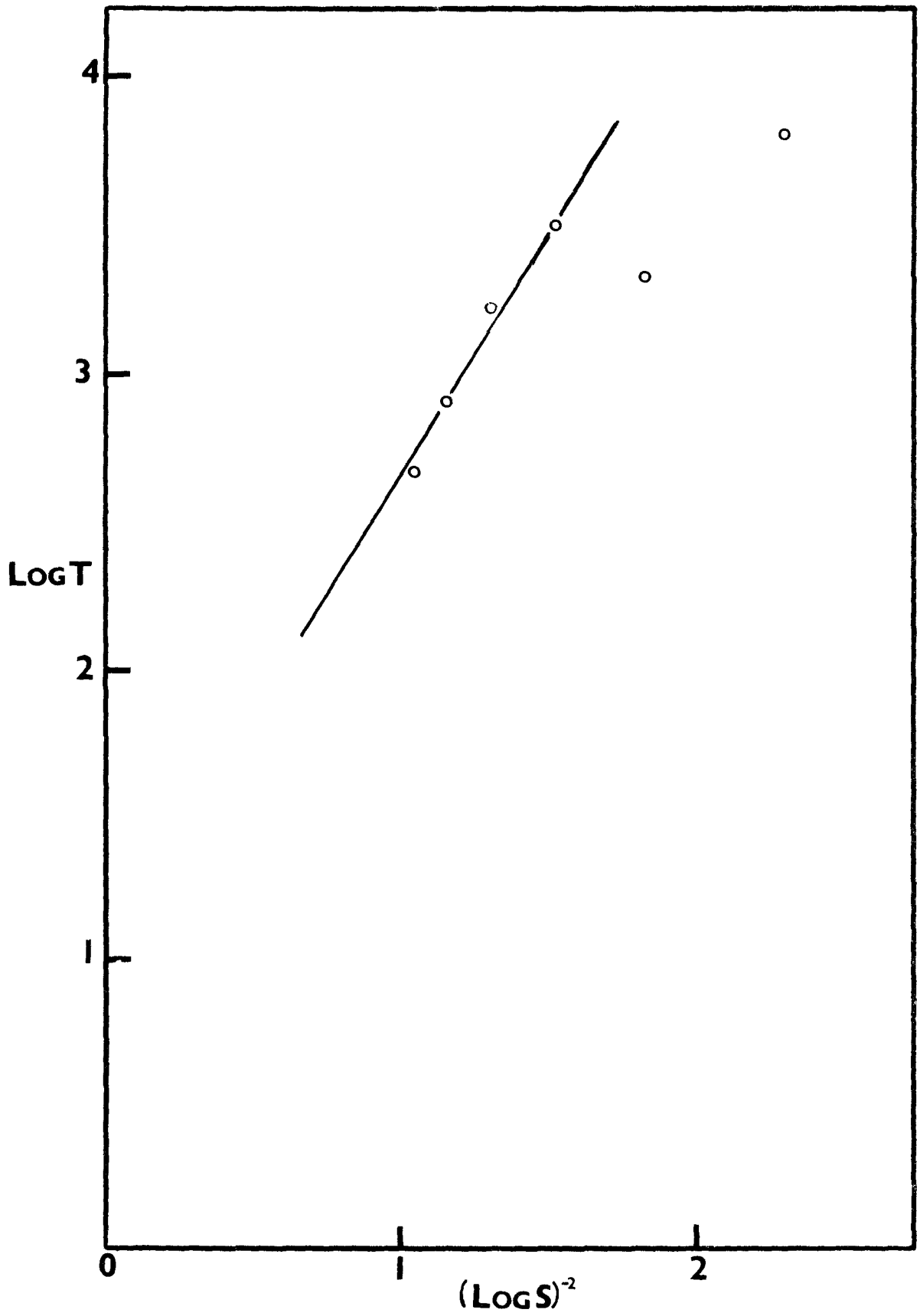
4
3
2
1
LogT
0
1
2
(LogS)$^{-2}$

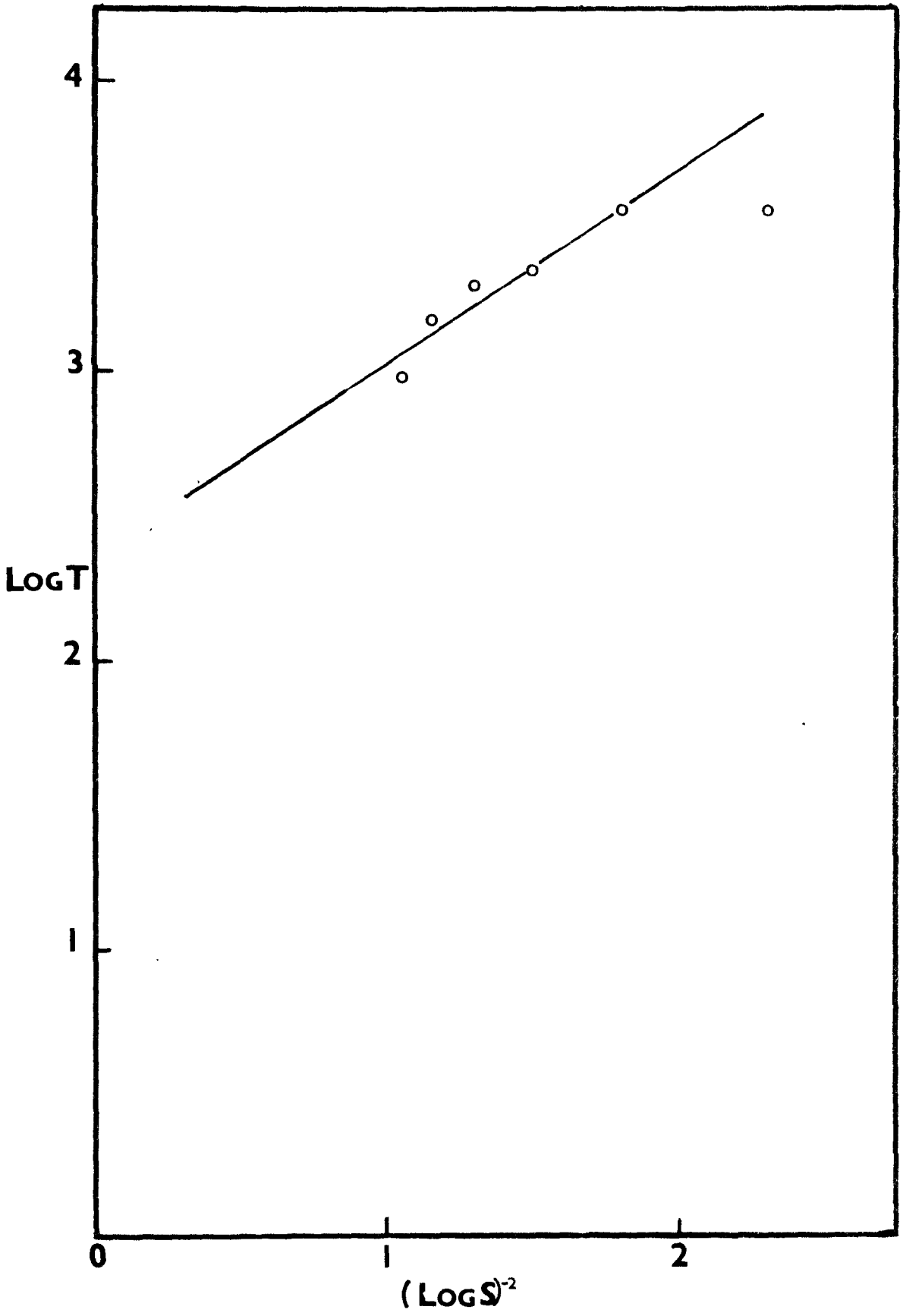
4
3
LogT
2
1
0
1
2
(LogS)$^{-2}$

curve BD is flatter than is shown, at least at low supersaturations. At high supersaturation, and assuming homogeneous nucleation, the mean embryo lifetime and the time for the nucleus to grow to detectable size will be constant if the same method of detection is used. If on the other hand the detection methods are different, one more sensitive than the other, the measured values of L_m will be different since t_1 (Fig. 1) will be different. L_m will be shorter for the more sensitive detection method. This explains the lower values for L_m in the fluorescence experiment as compared with similar values for the polarized light experiments at corresponding supersaturations.

The larger number of droplets which remained apparently without crystals in the polarized light experiments at low supersaturations can similarly be explained. The crystals which did not contain heteronuclei had longer L_m values and also the t_1 (Fig. 1) for the polarized light detection method is longer and so the crystals were not detected. The fluorescence method, with a short t_1 value, could detect most of these crystals at low supersaturation.

III.C.2. Calcium Tetracyanoplatinate(II)

III.C.2.a. Fluorescence method

The results of preliminary investigations showed that the crystals of calcium tetracyanoplatinate are fluorescent when the solution was dried on microscope slide and the crystals irradiated with ultraviolet radiation. The green crystals quickly turn dull red. When dispersions were prepared, however,

the crystals which appeared in the droplets were difficult to distinguish from the background when the slides were projected on the screen. Exposure time of up to 10 seconds did not produce any improvement in contrast. The crystals showed distinctly when photographed on microscope slides, but poorly or not at all in a droplet. This might be due to weak intensity of the fluorescence. For this reason, further study on the salt using the microscopic fluorescence technique was discontinued.

III.C.2.b. Results obtained using plane polarized light

Plane polarized light experiments were successfully used in studying nucleation of the salt from solution. A total number of 913 droplets, ranging in final diameter from 10 microns to 50 microns, were observed and analysed. Table 4 shows the subdivisions into supersaturation ranges, L_m for each range and the calculated rate of nucleation J. In Fig. 9 (plot of P vs L_n) there is a gradual increase in the gradient of the curves, as should be expected in homogeneous nucleation. As supersaturation increases so should the probability of nucleation. However, Figs. 10 and 11 show, if the analysis of the barium experiments is correct, at homogeneous and heterogeneous nucleation are occurring as in the other experiments. The linear relationship predicted by Equations 5 and 10 are borne out only at about $S \leqslant 4.2$. At values of $S \leqslant 4.2$ deviation from linearity is very strong. The supersaturation at which homogeneous nucleation is clearly predominant seems to occur at S = 4.2.

The median L_m for S = 2.0 is the same as for S = 4.2. This can be explained if it is assumed that homogeneous and heterogeneous nucleations are occurring simultaneously at low supersaturation, with the heterogeneous process predominating and thus making L_m low at low supersaturations. The supporting arguments are the same as given in Section III.C.1.a. and need not

TABLE 4

Data from studies of calcium salt.

Total number of droplets in subdivisions	Number with crystals	S	$(\log S)^{-2}$	Lm(T) sec	J $cm^{-3}sec^{-1}$	$\Delta p/\Delta t$
92*		<2				
22*		2±.2				
43	40	2.3	7.65	2880	7.0×10^5	4×10^{-4}
10*	10	2.5				
120	117	2.8±.2	5.00	3000	8.0×10^5	4×10^{-4}
136	134	3.2±.2	3.92	3000	1.2×10^6	5×10^{-4}
106	106	3.7±.2	3.10	3120	1.2×10^6	
150	150	4.2±.2	2.57	1920	1.4×10^6	6×10^{-4}
102	102	4.6±.2	2.28	2040	1.4×10^6	7×10^{-4}
47	47	5.0±.2	2.05	1560	1.6×10^6	8×10^{-4}
62	62	5.6±.2	1.79	1200	2.0×10^6	10×10^{-4}
23	23	6.2	1.59	600	3.3×10^6	17×10^{-4}

*Group of droplets not analysed.

Total number of droplets 913.

Mean radius 20 microns.

Fig. 8. Histogram of number of droplets nucleating with time for calcium salt. Method of detection: plane polarized light.

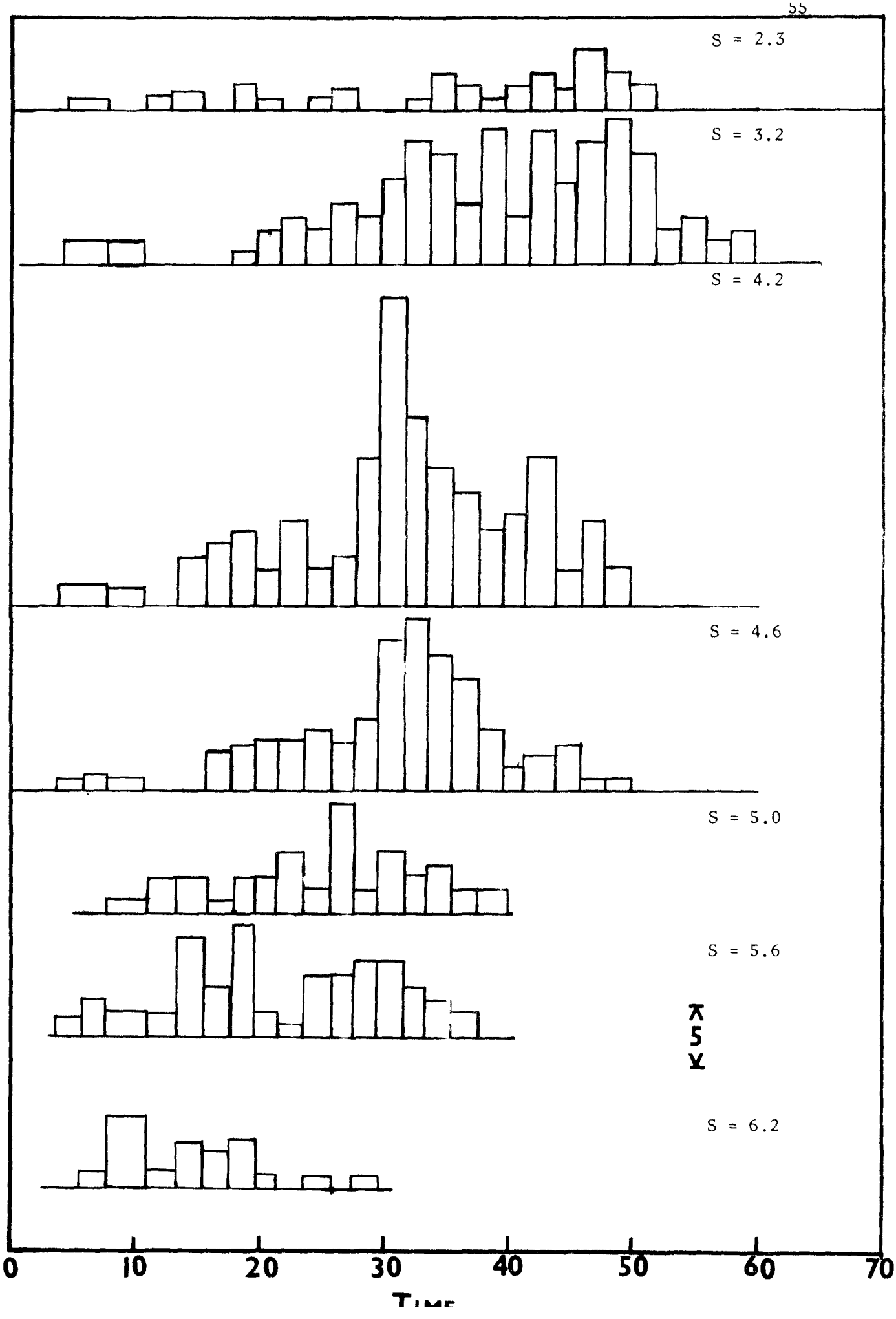
S = 2.3
S = 3.2
S = 4.2
S = 4.6
S = 5.0
S = 5.6
S = 6.2
0
10
20
30
40
50
60
70
TIME

Fig. 9. Plot of probability of nucleation with time for calcium salt.

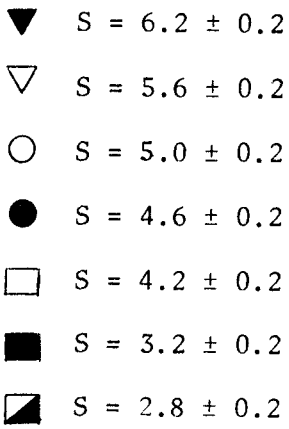

Note: Some points in the probability vs time curves were not used because the number of droplets involved were small.

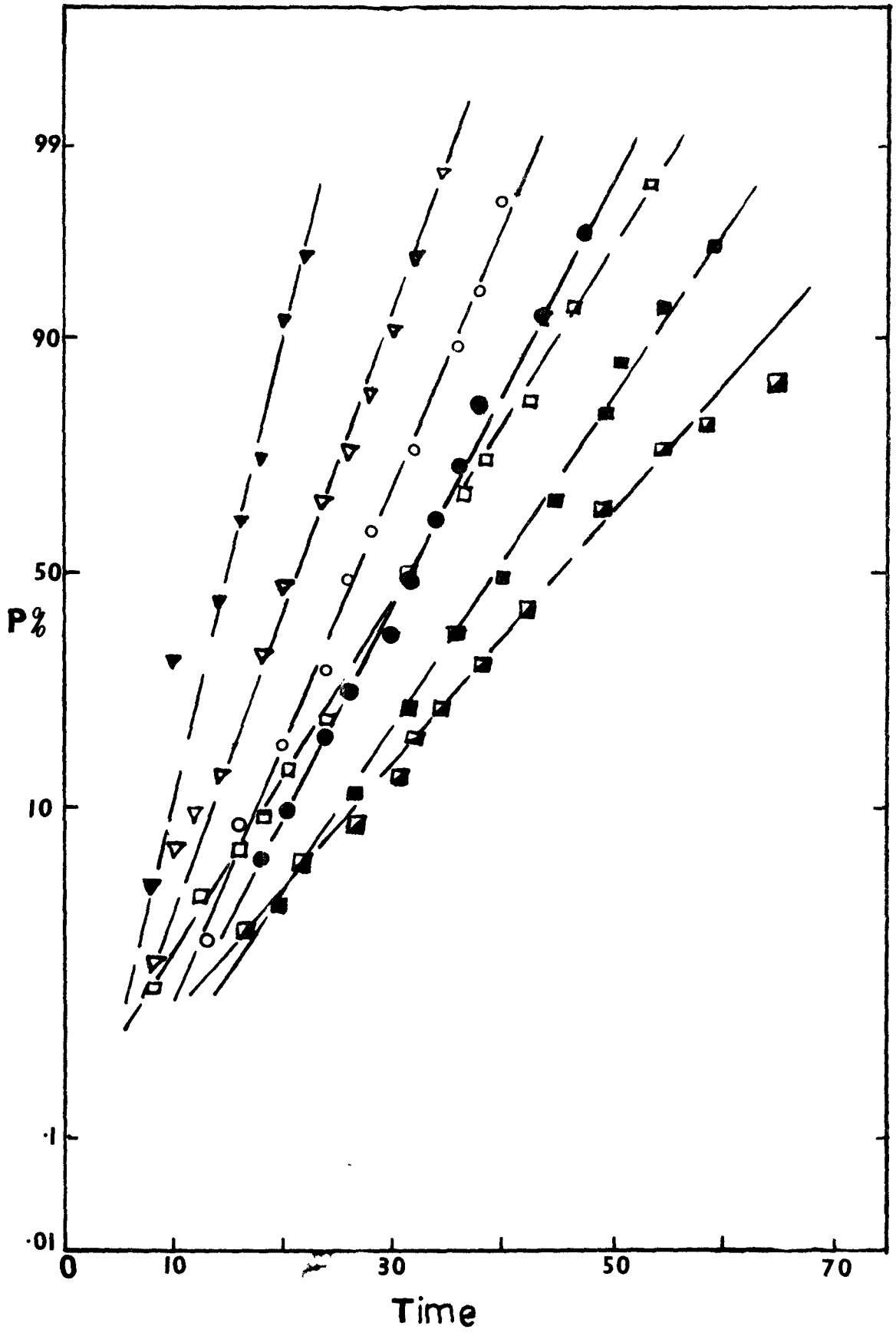
99
90
50
P%
10
·1
·01
0
10
30
50
70
Time

Fig. 10. A plot of log T vs $\log(1/\log S^2)$ for calcium salt.

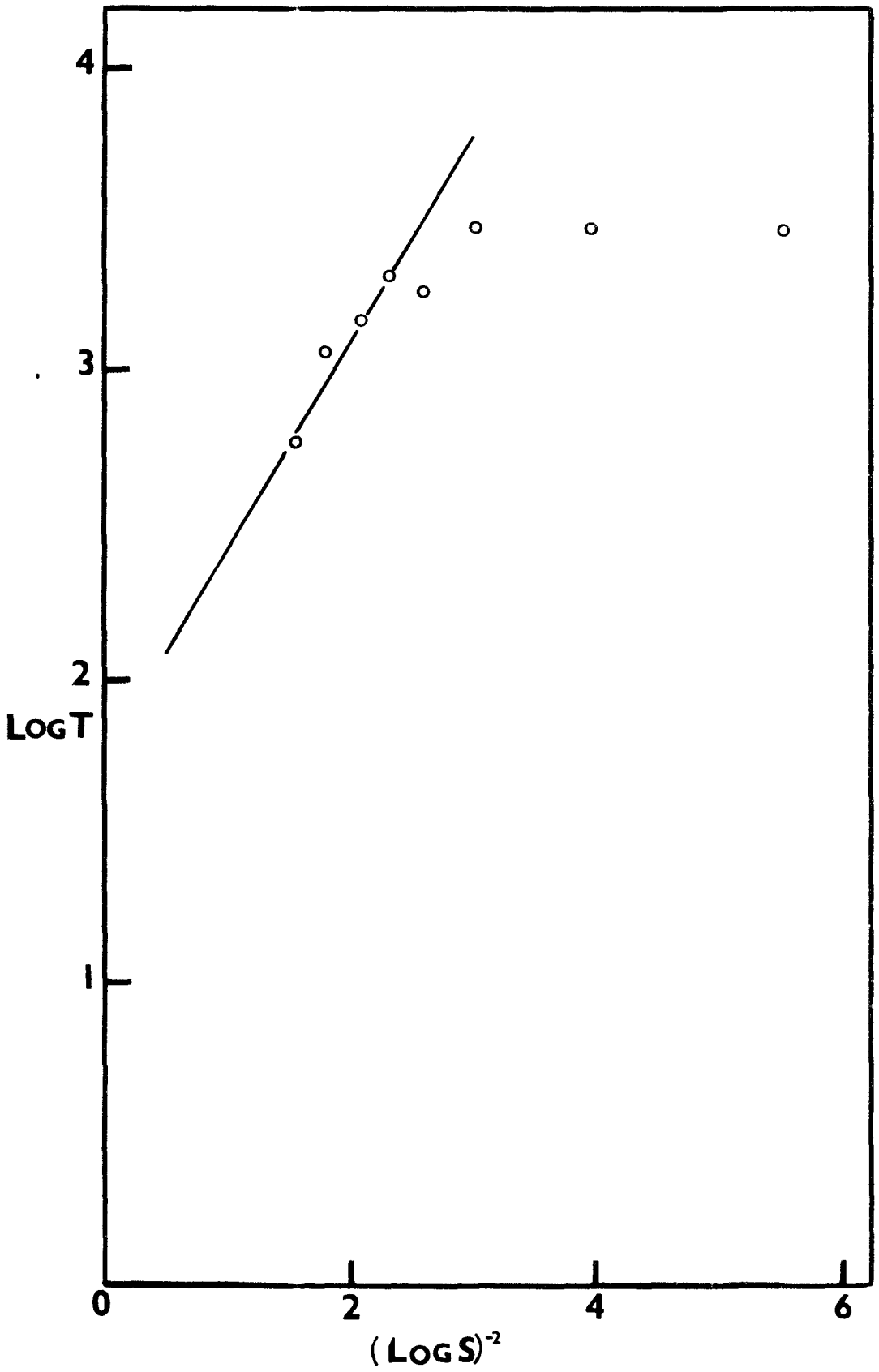
4
3
2
LogT
1
0
2
4
6
(LogS)$^{-2}$

Fig. 11. The plot of log J vs ($1/\log S^2$) for calcium salt.

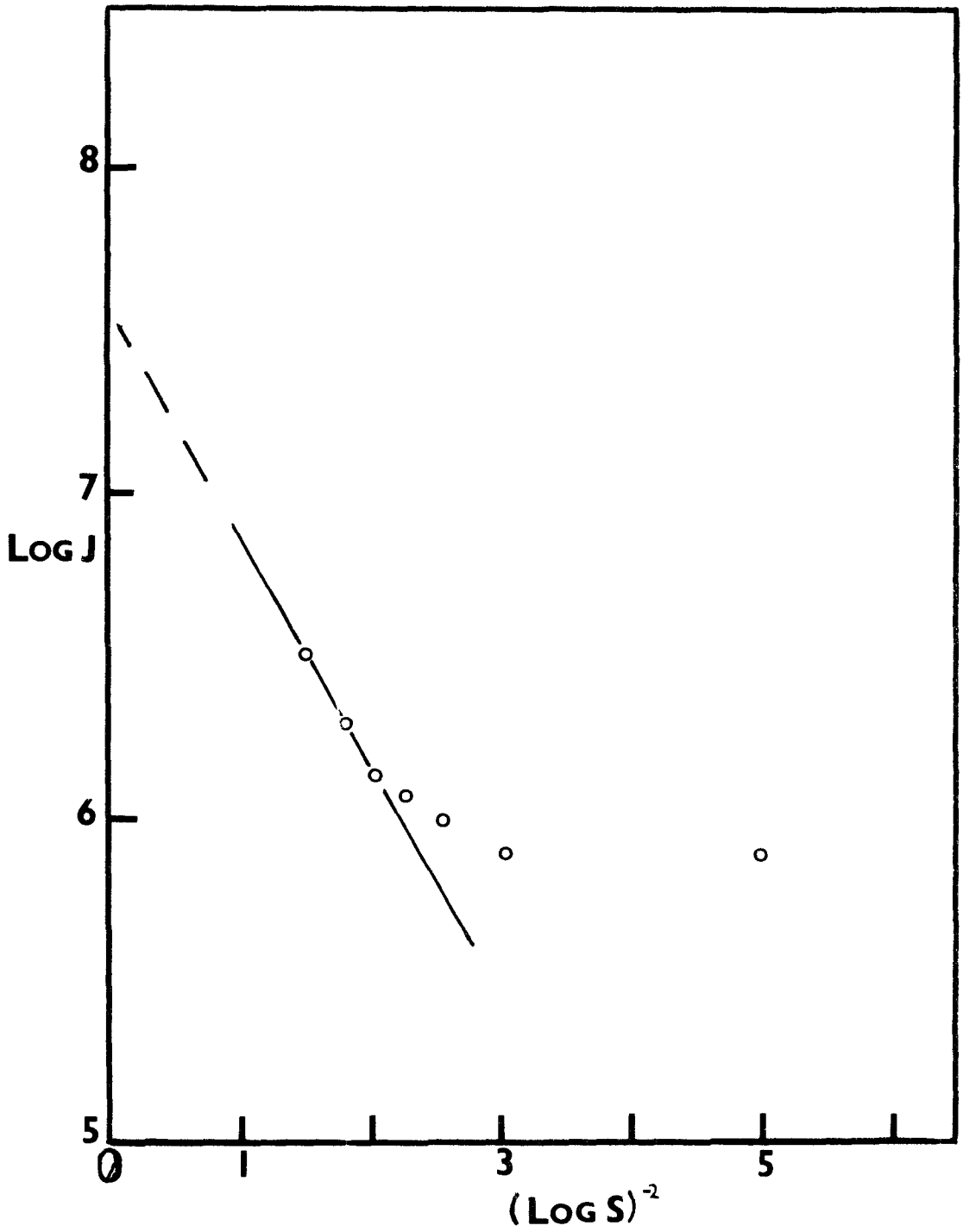
8
7
6
5
LOG J
0
1
3
5
(LOG S)$^{-2}$

be repeated here. The fact that Fig. 9 shows only single distributions - not the truncated type shown by the barium salts - may be interpreted to mean that one process might be taking place at low supersaturations and the other taking over at higher supersaturation. Whatever it is, the presence of one does not seem to affect the other.

Further discussions will be given later.

III.C.3. Magnesium Tetracyanoplatinate

III.C.3.a. Fluorescence method

The difficulty encountered with the use of fluorescence detection method in studying the magnesium salt was the same as that encountered with the calcium salt. The low intensity of the reddish fluorescence was difficult to record photographically even on relatively long exposures. When slide pictures were successfully obtained it was difficult to distinguish small crystals in droplets. In most instances, the whole droplet needed to crystallize before it could be distinguished from one with no crystals in it. Because of these difficulties only the data obtained by using plane polarized light for detection were analysed.

III.C.3.b. Results obtained using plane polarized light

Table 5 shows the total number of droplets analysed and the supersaturation range. The number of droplets (133) with supersaturation ratio below 1.5 were not analysed because a large number of them contained crystals even on the second slide, leading to suspicion that crystal formation was catalysed by agent(s) other than self-nucleation. Figs. 12 through 14 show the same characteristics as the corresponding figures for the barium salt. Good linearity is attained at $S \geq 3.0$, showing evidence of homogeneous nucleation. The interpretations are the same as those offered for the barium experimental

TABLE 5

Data from magnesium salt studies.

Total number of droplets in subdivisions	Number with crystals	S	$(\log S)^{-2}$	Lm(T) sec	J $cm^{-3}sec^{-1}$	$\Delta p/\Delta t$
133*		1.5				
35*	35	1.5±.2				
77	71	2.1±.2	9.63	600	2.9×10^{5}	3.3×10^{-4}
142	138	2.4±.2	6.92	720	2.9×10^{5}	3.3×10^{-4}
164	164	2.7±.1	5.37	720	4.9×10^{5}	3.5×10^{-4}
227	227	3.0±.1	4.39	480	5.3×10^{5}	3.6×10^{-4}
187	186	3.3±.2	3.72	600	9.0×10^{5}	6.3×10^{-4}
42	42	3.7	3.10	360	1.2×10^{6}	8.1×10^{-4}
33	33	4.2	2.58	360	1.5×10^{6}	10×10^{-4}

*Group of droplets not analysed.

Total number of droplets 1040.

Mean radius 18 microns.

Fig. 12. Histogram of number of droplets nucleating with time for magnesium salt. Method of detection: plane polarized light.

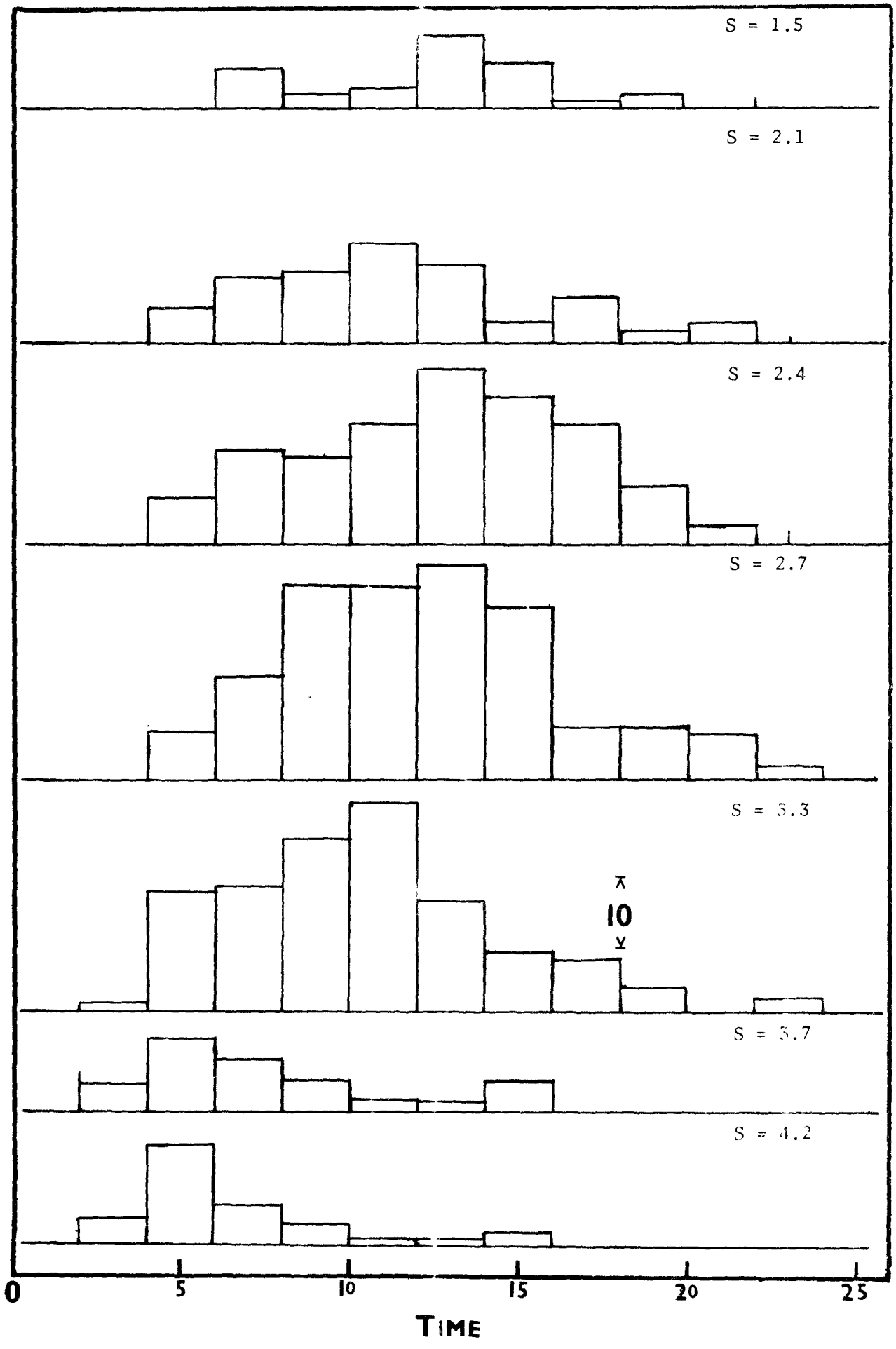
S = 1.5
S = 2.1
S = 2.4
S = 2.7
S = 3.3
$\bar{x}$
10
$\underline{x}$
S = 3.7
S = 4.2
0
5
10
15
20
25
TIME

Fig. 13. The probability of droplet nucleation with time for magnesium salt. Method of detection: plane polarized light.

Legend:

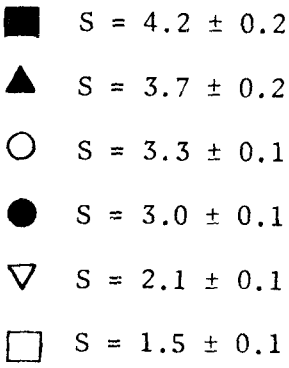

Note: Some points in the probability vs time curves were not used because the number of droplets involved were small.

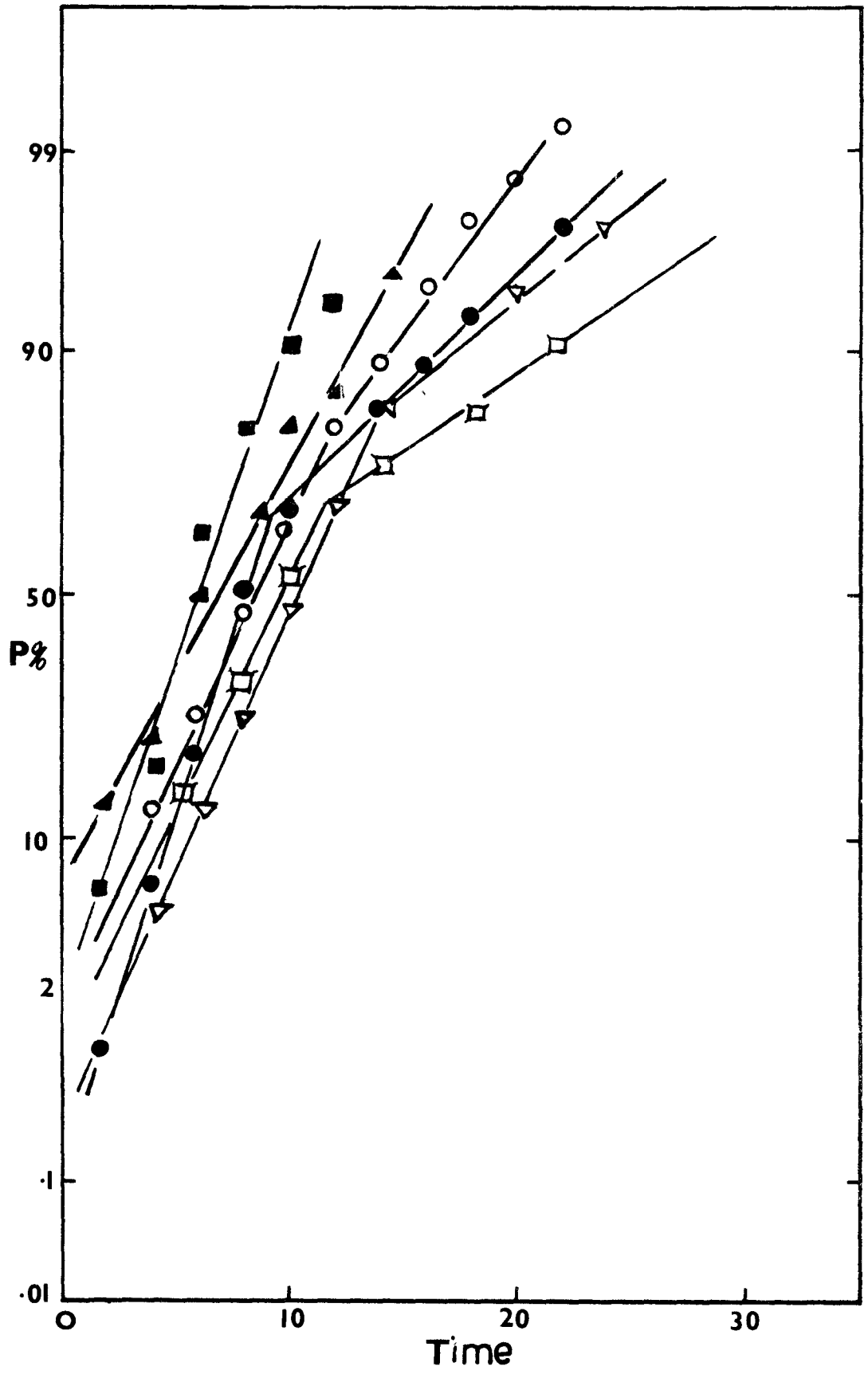
99
90
50
P%
10
2
·1
·01
0
10
20
30
Time

Fig. 14. Plot of log J vs $1/\log^2 S$ for magnesium salt.

Note: Some of these points corresponding to low supersaturation (or heterogeneous nucleation) were not used in these curves. For rationale see pages 42-49.

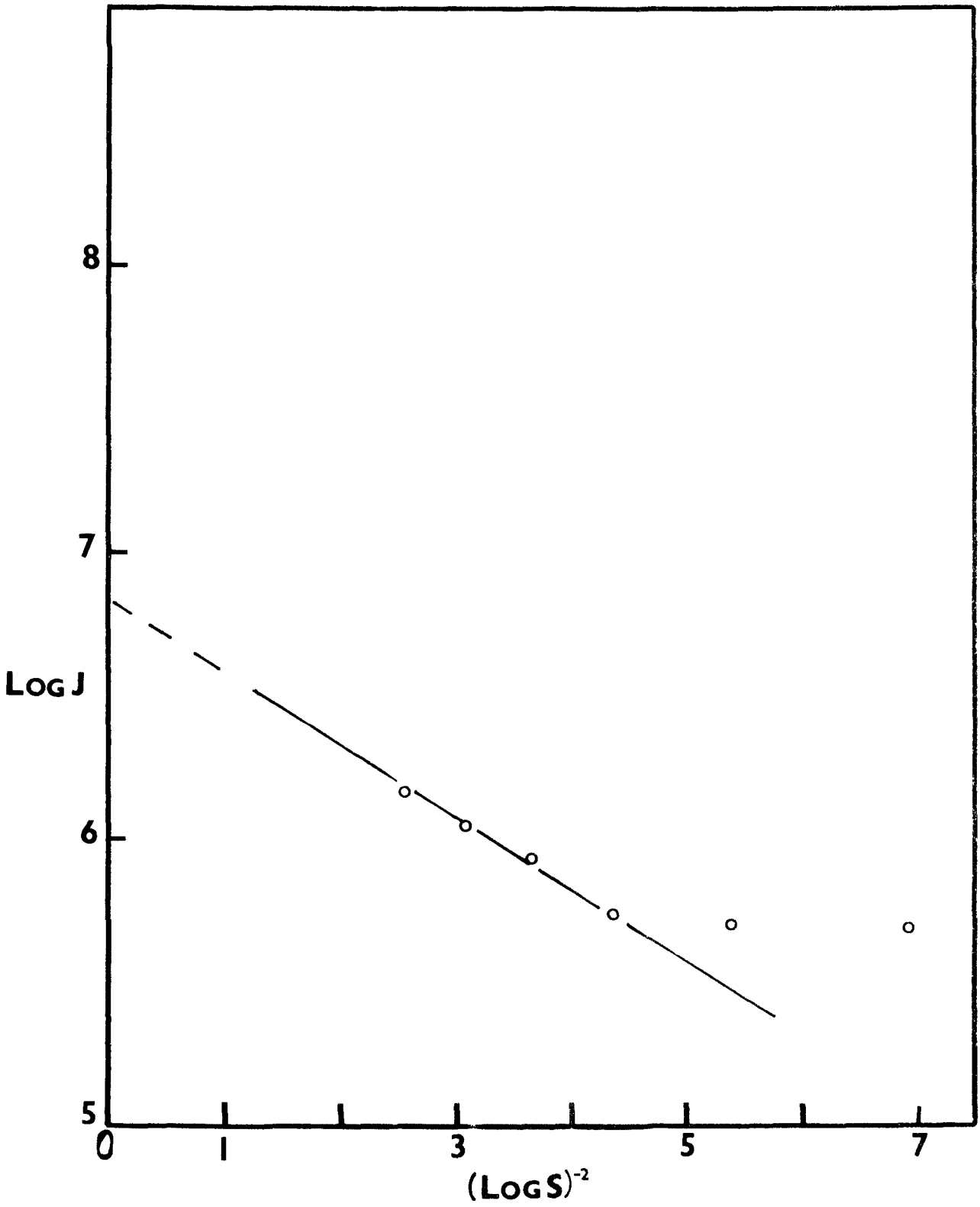
8
7
6
5
Log J
0
1
3
5
7
(Log S)$^{-2}$

Fig. 15. Plot of log T vs $(1/\log S^2)$ for magnesium salt.

Note: Some of these points corresponding to low supersaturation (or heterogeneous nucleation) were not used in these curves. For rationale see pages 42-49.

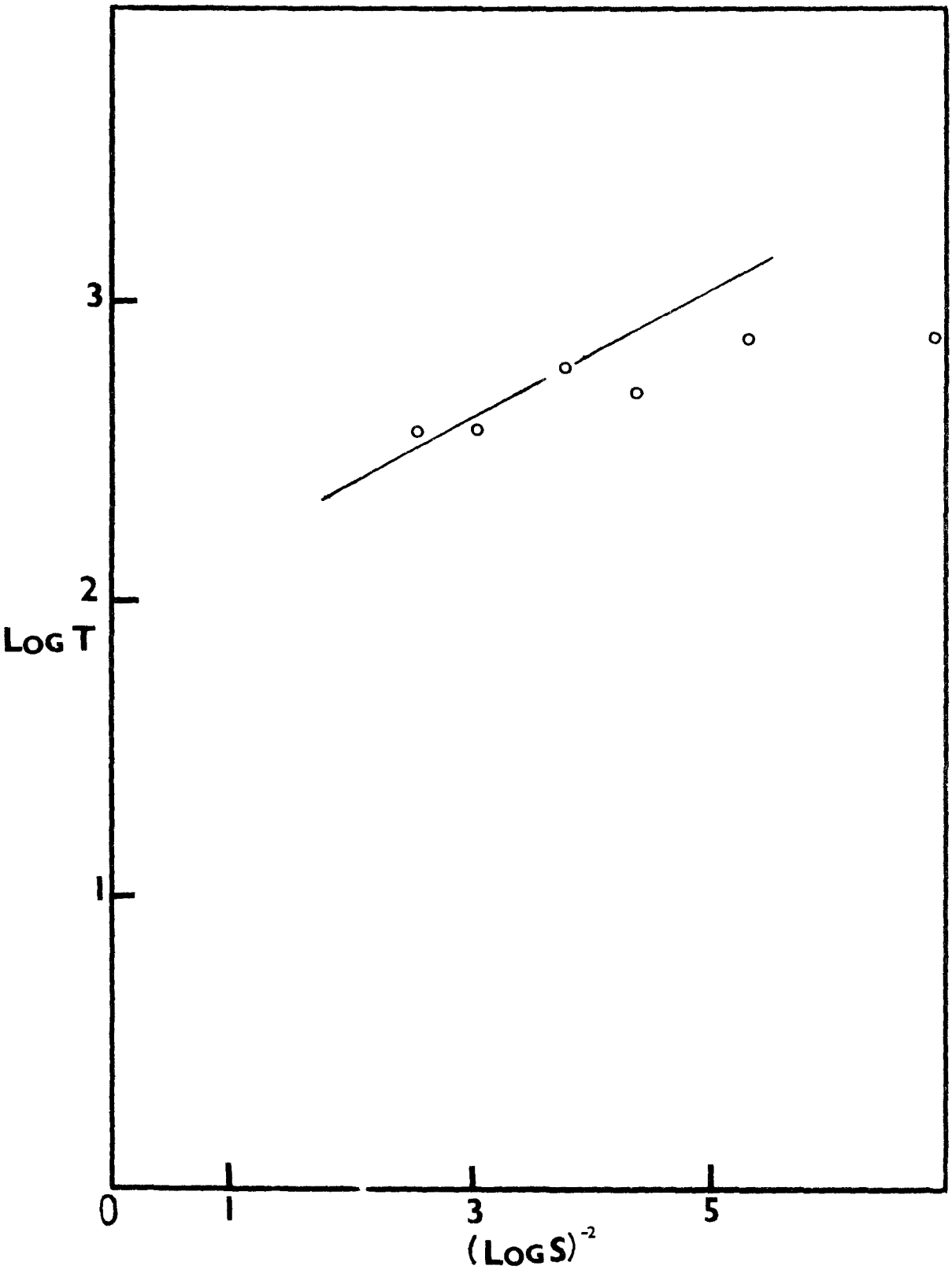
3
2
Log T
1
0
1
3
5
(Log S)$^{-2}$

results and are therefore not repeated here.

III.D. General Discussion

In this section, a discussion of the general aspects of the constants obtained using both the classical model of analysis and the mean lifetime of embryo model is given. This is because the compounds studied are of the same general nature. These constants are: A, the pre-exponential or kinetic factor, and σ, the interfacial energy between the forming phase and the mother phase. Table 6 shows these and other constants obtained.

III.D.1. Evaluation of the Fluorescent Method of Detection

The only data which allows for evaluation of the fluorescent method is the values of the mean lifetime of embryo at high supersaturation ratios. Compared with values obtained from the plane polarized light experiments on the same salt at the same supersaturations, the mean lifetime values of the fluorescence experiment are lower. Again inspection of Tables 2 and 3 shows that crystals were detected in relatively more droplets at low supersaturations with the fluorescent technique than with plane polarized method of detection. Taken together these seem to indicate that the fluorescent method of detection is a more efficient method of crystal detection. We think, however, that more study is needed for complete evaluation of the technique.

III.D.2. The Kinetic Factor

The experimental values obtained for the pre-exponential or kinetic factor for the barium, calcium and magnesium salts are well below the theoretical value of $10^{30\pm3}$ predicted by the classical theory, by comparable to experimental values in the literature (Table 7). The theoretical value was calculated for the same assumptions as that for nucleation from the melt. It has been usual to assume that similar values can be used for nucleation of ionic salts from aqueous solutions [56].

TABLE 6

Summary of parameters obtained using both the classical model and the mean lifetime model of analysis.

Compound	Detection method	σerg cm^{-2}	σerg cm^{-2} [b]	n^*	r^* Å	log A
Barium salt	Polarized light	11.00	9.60	47	13.2	8.70
	fluorescence	15.4	13.0	40	12.1	10.2
Calcium salt	Polarized light	9.00	8.70	49	13.7	7.60
Magnesium salt	Polarized light	8.10	6.90	74	14.3	6.80

[b] Interfacial energy values obtained from the gradient of log T - $(\log S)^{-2}$ curve.

log A is experimental.

Values of n^* and r^* obtained using $\log S_{J=1}$ from log J vs $(\log S)^{-2}$ plot.

TABLE 7

Some values of log A and σ determined experimentally

(from literature)

Compound	log A	σ^a erg cm^{-1}	Method	r^* (Å)	Reference
$NH_4C\ell$	3.37	35	DT[a]		60,62
		66	DT	9.0	61
NH_4Br	2.96		DT		60
KNO_3	5.31	57	DT		
$K_2Cr_2O_7$	5.6	72	DT	8.6	62
$Pd(C_7H_{11}N_2O_2)_2$	6.7	23	DT	16	63
$Pd(C_6H_9N_2O_2)_2$	12.0	36	DT	12	63
$Ni(C_7H_{11}N_2O_2)_2$	7.3	34	DT	12	63
$Ni(C_6H_9N_2O_2)_2$	8.0	29	DT	14	63
$BaSO_4$	22.3	151	DM	4.3	59
$SrSO_4$	11.8	70	DM	5.1	59,64
$PbSO_4$	20.0	119	DM		59
CaF_2	13.5	140	DM		59

DT = droplet technique

DM = direct mixing technique

[a] σ was calculated by assuming log A = 30 and J = 1 $cm^{-3}sec^{-1}$.

Values obtained experimentally, however, are considerably lower. This is as should be expected. Firstly, the blocking tendency of ionic charge and water of solvation is not accounted for in the theoretical calculations. These factors will impede and subsequently slow down the rate of addition of monomers to embryos. A slow rate of addition will lower the kinetic factor.

Secondly, in solution it may be necessary to overcome (at least partially) the solvation of the monomers before nucleation can take place. Thus it would be expected that both the energy barrier to desolvation and the large entropy changes coupled with the blocking tendency of escaping solvent molecules will lower A.

Thirdly, in high supersaturated solutions, viscosity is high, resulting in increase in the energy barrier to active transport.

And finally, the possibility of embryos being charged in ionic solution must be considered. In such a situation the presence of electrical double layer around the embryo will have a blocking tendency, resulting in a low kinetic value.

The theoretical value of the kinetic constant is a subject of animated discussion in the literature. The number of molecules colliding with a boundary surface per unit time has been evaluated by assuming that the molecule which is in contact with the surface of the nucleus is in transition state. This value of the collision flux, incorporated into the expression for A, is "in the nature of a plausible guess which can be used in default of other estimates" [57].

The values obtained in this work are similar, at least in order of magnitude, to values reported in the literature. These values, especially those reported for droplet experiments, are usually below 10^{10}.

III.D.3. The Interfacial Energy

The values of the interfacial energy reported for all the salts were calculated in two different ways. One value was obtained from the mean lifetime model and the other directly from the classical model. The degree of similarity between these sets of values gives much confidence to the order of magnitude one should expect.

Our values have not been compared with values reported in the literature because of differences in method of calculation. In the literature the values of σ are calculated by assuming some value of A and J = 1 $cm^{-3}sec^{-1}$. This was not done here because the same assumption cannot be made for the mean half-life model.

Walton [58] has predicted values of 150-200 ergs cm^{-1} for ionic crystals in solution. This is surprising in view of the fact that a lot of ionic crystals formed from aqueous solution do so with water of crystallization. For example, the salts studied crystallize with five molecules of water. In such a situation the Gibb's surface of tension is even difficult to imagine. The low value obtained for the interfacial energy is therefore reasonable.

III.E. Errors

The major source of error in these experiments is the measurement of the diameter of the droplet. The maximum error here is estimated as about 10% leading to a maximum error of about 15% in the computation of the supersaturation ratio. But because the supersaturation ratio used is a mean of a large aggregate this error is probably smaller than the 15% estimate. The assumption and the inadequacies mentioned in the introduction make this error acceptable.

III.E.1. Summary

1. A microscopic fluorescence method has been successfully used in the

study of nucleation from homogeneous nucleation, and has been shown to be an efficient method of detection.

2. Experimental evidence has been provided for the mean lifetime of the embryo at any given supersaturation.

3. Frisch and Carlier expression for the mean lifetime has been used for the first time to analyse experimental data successfully.

4. It has been shown that growth rate of a small crystallite in solution is slower than previously assumed.

5. The values of the kinetic factor obtained (10^7 - 10^{10} $cm^{-3}sec^{-1}$) for the components has been compared with literature values and reasons given for their being acceptable values.

6. Values for the interfacial free energy (σ) have been obtained for the compounds studied by two models of analysis. The similarity between the two sets of results have been commented upon.

III.E.2. Suggested Future Work

The results of this work have shown that the fluorescent method of detection is an efficient and useful addition to the arsenal of methods to assault the problem of nucleation from solution. In its present state - microscopic observations and photographic recording, not to mention the tedius counting and measurement processes - has all the difficulties of the polarizing microscopic technique. But it has a big advantage - it could be automated.

Also, future efforts should be directed at finding or preparing compounds which have the properties stated in Chapter 1 and to detecting the fluorescence emitted by the forming phase by some means other than photographic film. It has been our suspicion that the accuracy in this method will depend upon the sensitivity of the recording device.

APPENDIX I

CALCULATION OF RATE OF NUCLEATION FROM DROPLET EXPERIMENTS ON SUPERCOOLED WATER

The probability of crystallization taking place in a volume V within the time interval t to t+dt may be written as $Vf(\bar{I}s)dt$ where $f(\bar{I}s)$ is a function of the supercooling $\bar{I}s$. If the supercooling in a large number N, of identical but isolated drops of volume V, is the same for all the droplets, then the probability of crystallization taking place in the volume V during the time interval 0 to t, is

$$P(V,t) = N_t/N \qquad 11a$$

where N_t = number of drops frozen at time t.

The number of crystallized drops during the interval 0 to t+dt is

$$N_{t+dt} = N_t + (N - N_t)Vf(\bar{I}s)dt \qquad 11b$$

Dividing both sides by N gives

$$P(V,t+dt) = P(V,t) + \{1 - P(V,t)\}Vf(\bar{I}s)dt \qquad 11c$$

But $$P(V,t+dt) = P(V,t) + dt\,\frac{\partial P}{\partial t}(V,t) \qquad 11d$$

hence $$\frac{\partial P}{\partial t}(V,t) = \{1 - P(V,t)\}Vf(\bar{I}s) \qquad 11e$$

or $$\ln\{1 - P(V,t)\} = -V\int_0^t f(\bar{I}s)dt \qquad 11f$$

Mason and Kuhns [65] have shown that $\int f(\bar{I}s)$ can be identified with $J(\bar{I}s)$, the rate of formation of critical size nuclei.

Thus $$\ln(1 - P) = -V\int J(\bar{I}s)dt \qquad 11g$$

or $$J(\bar{I}s) = \frac{1}{1-P} \cdot \frac{1}{V} \cdot \frac{dP}{dJ_s} \cdot \frac{dJ_s}{dt} \qquad 11h$$

$$J = \frac{1}{1-P} \cdot \frac{1}{V} \cdot \frac{dP}{dt} \cdot \qquad 11i$$

The only unknown on the right hand of Equation 11i, P, could be calculated and dP/dt could also be obtained at a given supersaturation.

APPENDIX II

The problem of concentration of any component in a droplet located in a medium in which one component is transferring from the droplet to the surrounding medium. Physical transfer is assumed, i.e., no chemical reaction at the droplet/bulk phase interface, and that transfer corresponds to transfer from a spherical droplet into a stagnant medium.

It is assumed that:

1. the concentration of the transferring component in the bulk phase remains constant during the time interval (small amount of transferring phase actually transferred);
2. the concentration at the droplet/bulk phase interface corresponds to equilibrium conditions;
3. the droplet has a uniform concentration; and
4. the equilibrium concentration for the transferring component is independent of the non-transferring component in the droplet (this is expected to be realistic for low concentrations).

Nomenclature

C_∞ is concentration in the bulk solution.

C^* is the concentration in silicone (bulk) phase at the surface of the droplet (this corresponds to saturated silicone concentration).

C_A is equilibrium concentration of solute in water.

D_o is the diameter at a time t = 0.

Suffixes A and L correspond to the non-transferring component (solute), and the liquid transferring (solvent).

$$C_A = m_A/(m_A/\rho_A + m_L/\rho_L) \qquad 1$$

C_A is in gm-moles/unit volume, and

ρ_A and ρ_L are molar densities.

Equation (1) assumes ideal solution $\Sigma \cdot \nu_i = V_T$. Differentiating (1) with respect to time, and noting that m_A is constant, we have

$$\frac{dC_A}{dt} = d[m_A/(m_A/\rho_A + m_L/\rho_L)] = d[(m_A/V_A + V_L)/dt] = -m_A(V_A + V_L)^{-2} \frac{dV_L}{dt} \quad (2)$$

where V_A = volume of component A, and

V_L = volume of component L.

Now, dV_L/dt is related to mass transfer rate of water from droplet

$$\frac{dm_L}{dt} = - k_c \pi D^2 (C^* - C_\infty) \quad (3)$$

where k_c is a mass transfer coefficient given by

$$\frac{Dk_c}{D_{BA}} = 2 \quad (4)$$

where D_{BA} is diffusion coefficient of L in cm^2/sec,

D is droplet diameter in cm, and

k_c is in moles transferred/(unit area).

Equation (4) arises out of a solution of the basic diffusion equation in spherical coordinates.

From (3) $$\rho_L \frac{dV_L}{dt} = -k_c \pi D^2 (C^* - C_\infty) \quad (5)$$

But $$\frac{dV_L}{dt} = \frac{dV_T}{dt} = \frac{-k_c \pi D^2}{\rho_L} (C^* - C_\infty)$$

and $$V_T = \frac{\pi D^3}{6},$$

so $$\frac{dV_T}{dt} = 3D^2 \frac{\pi}{6} \frac{dD}{dt} \quad (6)$$

hence $$\frac{dD}{dt} = \frac{-k_c(C^* - C_\infty)}{\rho_L} \tag{7}$$

Substituting (4) in (7), we have

$$\frac{dD}{dt} = -\frac{4D_{BA}}{\rho_L D}(C^* - C_\infty) \tag{8}$$

$$\int_{D_o}^{D} 2D\,dD = -\int_{o}^{t} \frac{8D_{BA}}{\rho_L}(C^* - C_\infty)\,dt \tag{9}$$

Hence $$D_o^2 - D^2 = \frac{8D_{BA}}{\rho_L}(C^* - C_\infty)t$$

or $$D^2 = -D_o^2 - \frac{8D_{BA}}{\rho_L}(C^* - C_\infty)t$$

or $$D^2 = D_o^2 - k_2 t \tag{10}$$

where k_2 is a constant if D_{BA}, ρ_L, $(C^* - C_\infty)$ are constants.

Referring to Equation (2)

$$\frac{dC_A}{dt} = -m_A(V_T)^{-2}\frac{dV_L}{dt}$$

$$V_T = \frac{\pi D^3}{6}, \text{ hence } \frac{dV_L}{dt} = \frac{dV_T}{dt} = 3D^2\,\frac{\pi}{6}\,\frac{dD}{dt}$$

$$\frac{dC_A}{dt} = -m_A \cdot \left(\frac{6}{\pi}\right)^2 \cdot \frac{1}{D^6} \cdot 3D^2\,\frac{\pi}{6}\,\frac{dD}{dt}$$

Substituting for dD/dt from (8), we have

$$\frac{dC_A}{dt} = -m_A\left(\frac{6}{\pi}\right) \cdot \frac{1}{D^4} \cdot 3\left[-\frac{4D_{BA}}{\rho_L D} \cdot (C^* - C_\infty)\right]$$

$$= m_A \cdot \frac{72}{\pi} \cdot \frac{D_{BA}}{\rho_L}(C^* - C_\infty) \cdot \frac{1}{D^5}$$

Hence $$\frac{dC_A}{dt} = K_1 \frac{1}{D^5}. \qquad (11)$$

Using Equation (10) and integrating

$$\int_{C_{AO}}^{C_A} dC_A = \int_o^t K_1 \frac{1}{(D_o^2 - k_2 t)^{5/2}} dt$$

$$= -\frac{k_1}{k_2} d \frac{(D_o^2 - k_2 t)}{(D_o^2 - k_2 t)^{5/2}}$$

$$C_A \int_{C_{AO}}^{C_A} = \frac{2}{3} \frac{k_1}{k_2} \frac{1}{(D_o^2 - k_2 t)^{3/2}} \int_o^t$$

$$C_A - C_{AO} = \frac{2}{3} \frac{k_1}{k_2} \left[\frac{1}{(D_o^2 - k_2 t)^{3/2}} - \frac{1}{D_o^3} \right] \qquad (12)$$

Equation (12) relates concentration for every droplet of initial diameter D_o. It is to be noted that concentration will be different for all droplets of different sizes at any time since concentration depends on initial drop size.

Substituting in (12) for values of k_1 and k_2, we have

$$C_A - C_{AO} = \frac{2}{3} \frac{m_A \cdot \frac{72}{\pi} \cdot \frac{D_{BA}}{\rho_L} (C^* - C_\infty)}{8 \frac{D_{BA}}{\rho_L} (C^* - C_\infty)} \left[\frac{1}{\{D_o^2 - 8 \frac{D_{BA}}{\rho_L} (C^* - C_\infty) t\}^{3/2}} - \frac{1}{D_o^3} \right]$$

$$= \frac{6 m_A}{\pi} \left[\frac{1}{(D_o^2 - k_2 t)^{3/2}} - \frac{1}{D_o^3} \right]$$

But $$C_{AO} = \frac{6 m_A}{\pi D_o^3}$$

hence $$\frac{C_A}{C_{AO}} = 1 + D_o^3 \left[\frac{1}{(D_o^2 - k_2 t)^{3/2}} - \frac{1}{D_o^3} \right]$$

or $$\frac{C_A}{C_{AO}} = \frac{D_o^3}{[D_o^2 - k_2 t]^{3/2}}$$

But $S = \frac{C_A}{C_{AO}}$ (supersaturation ratio S).

$$\therefore \quad S = \frac{D_o^{\,3}}{[D_o^{\,2} - k_2 t]^{3/2}}$$

APPENDIX III

Sample data showing dependence of nucleation probability with time.

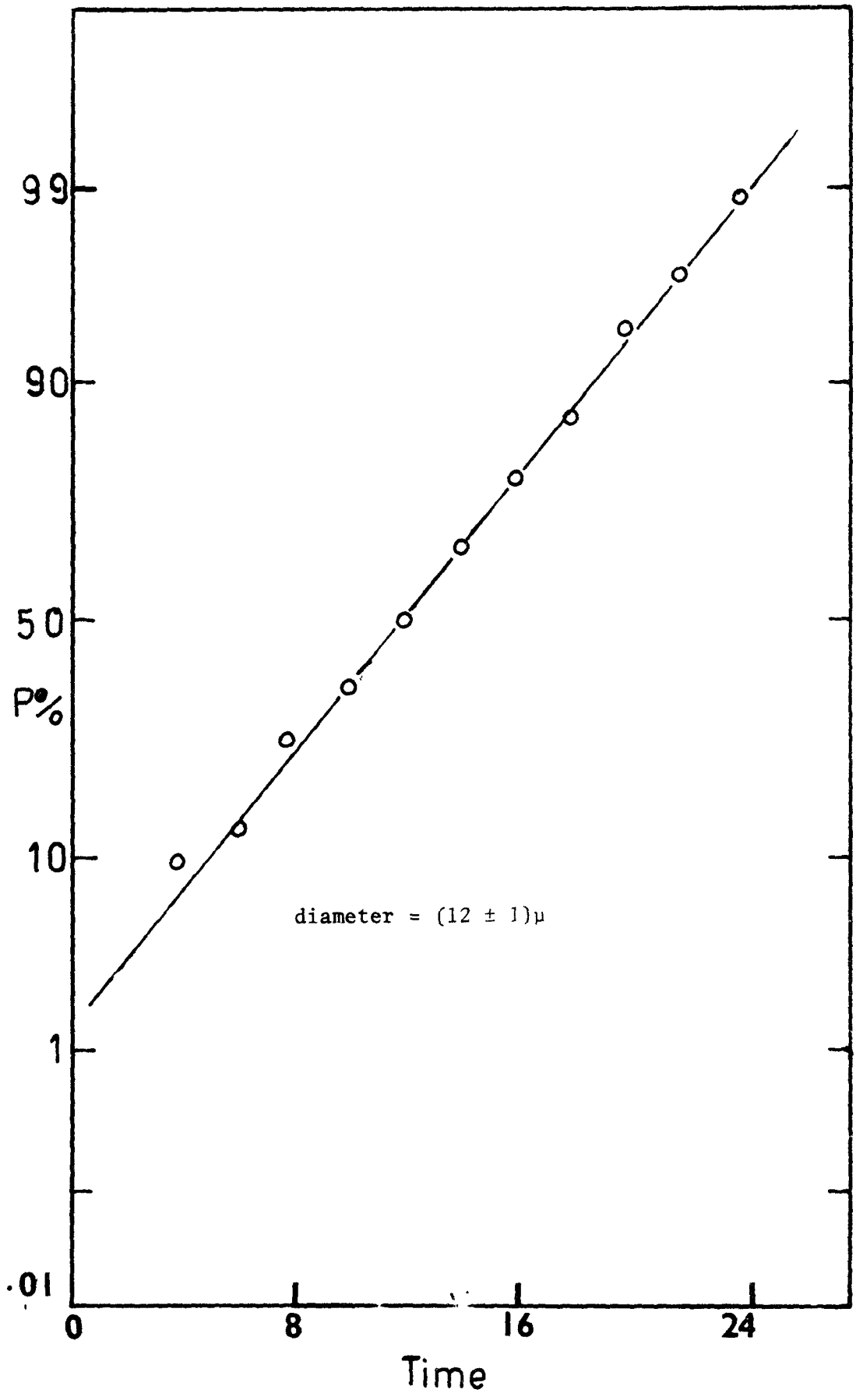

3a

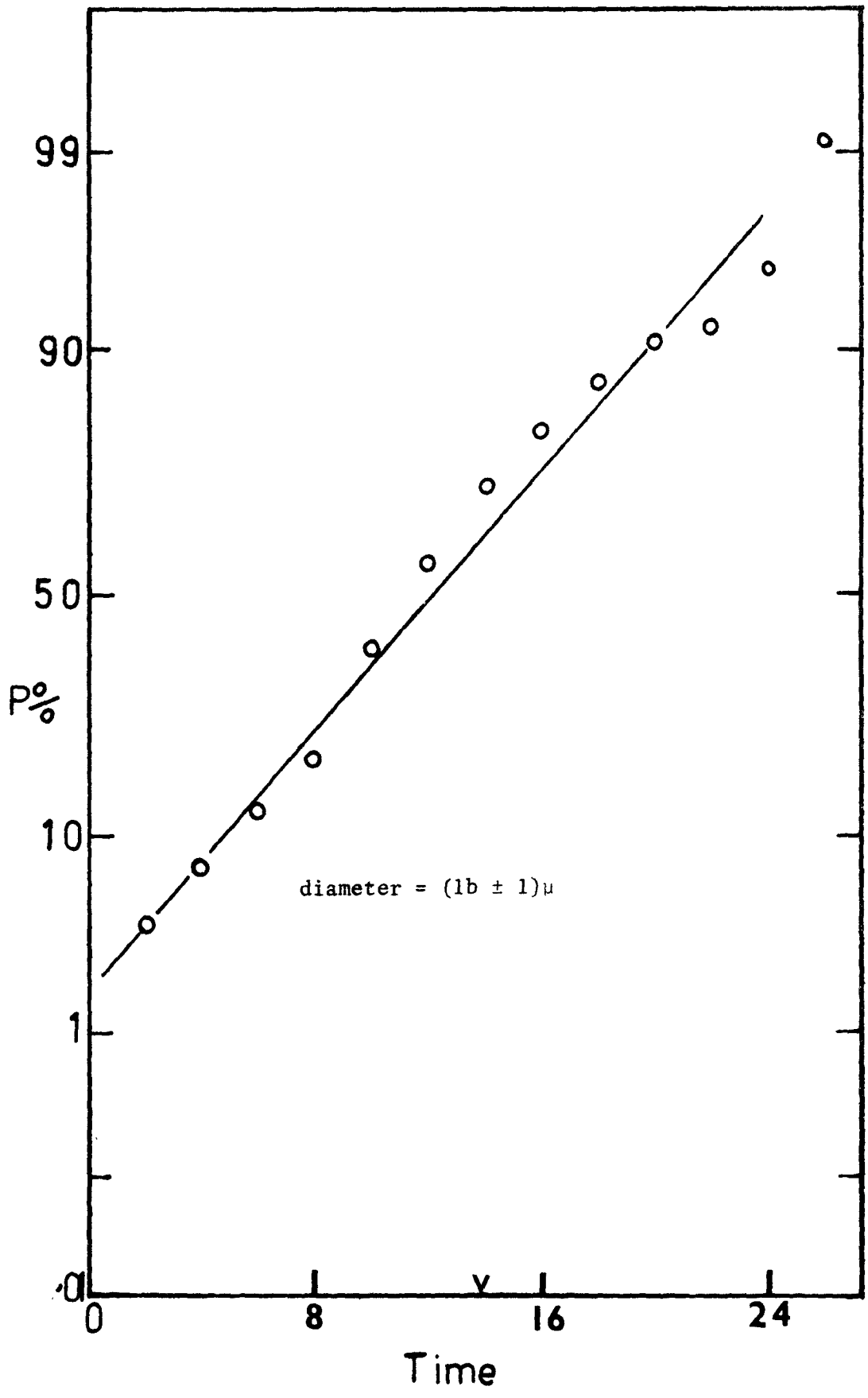

3b

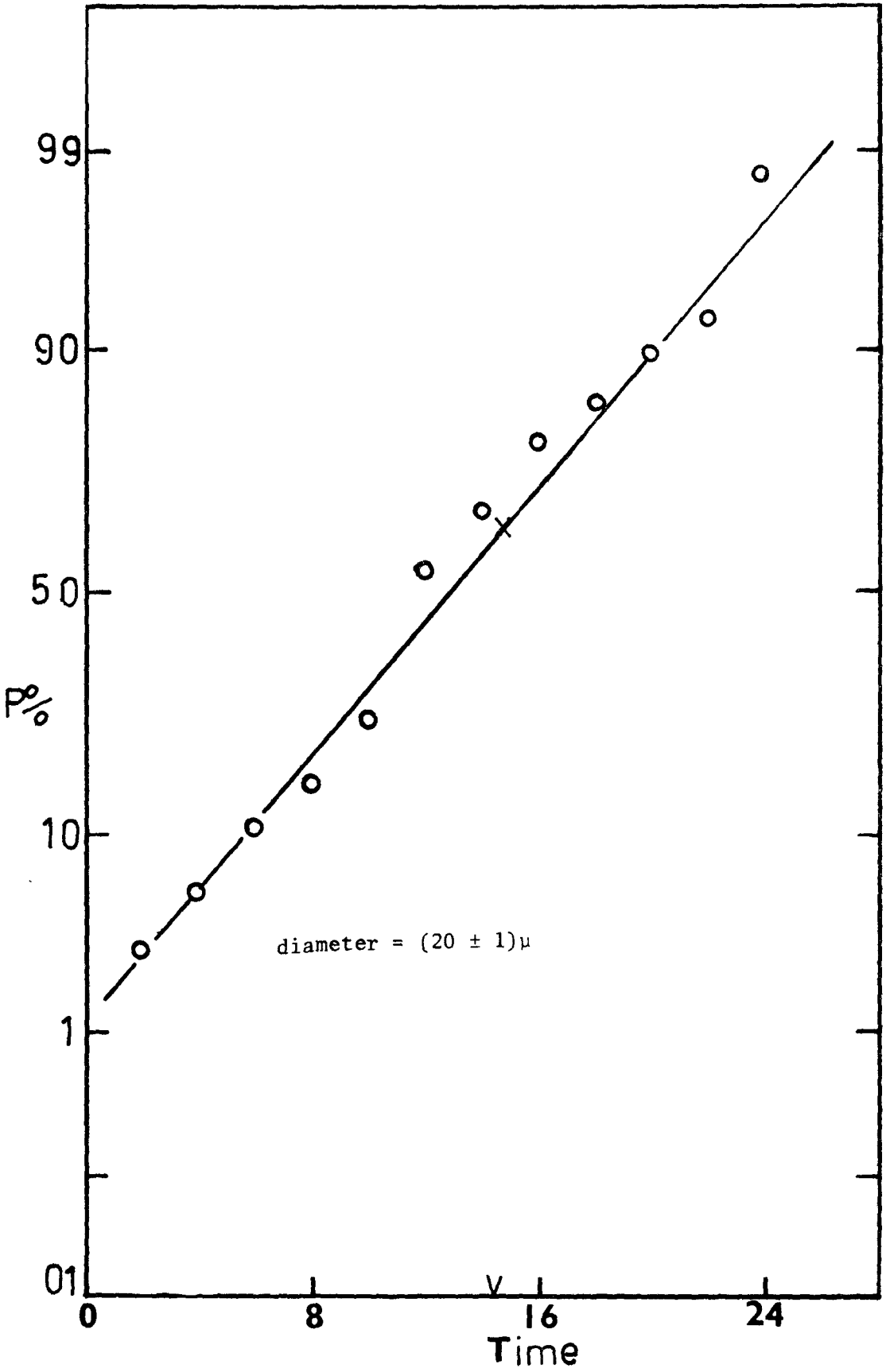
99
90
50
P%
10
1
01
0
8
16
24
Time
diameter = (20 ± 1)μ

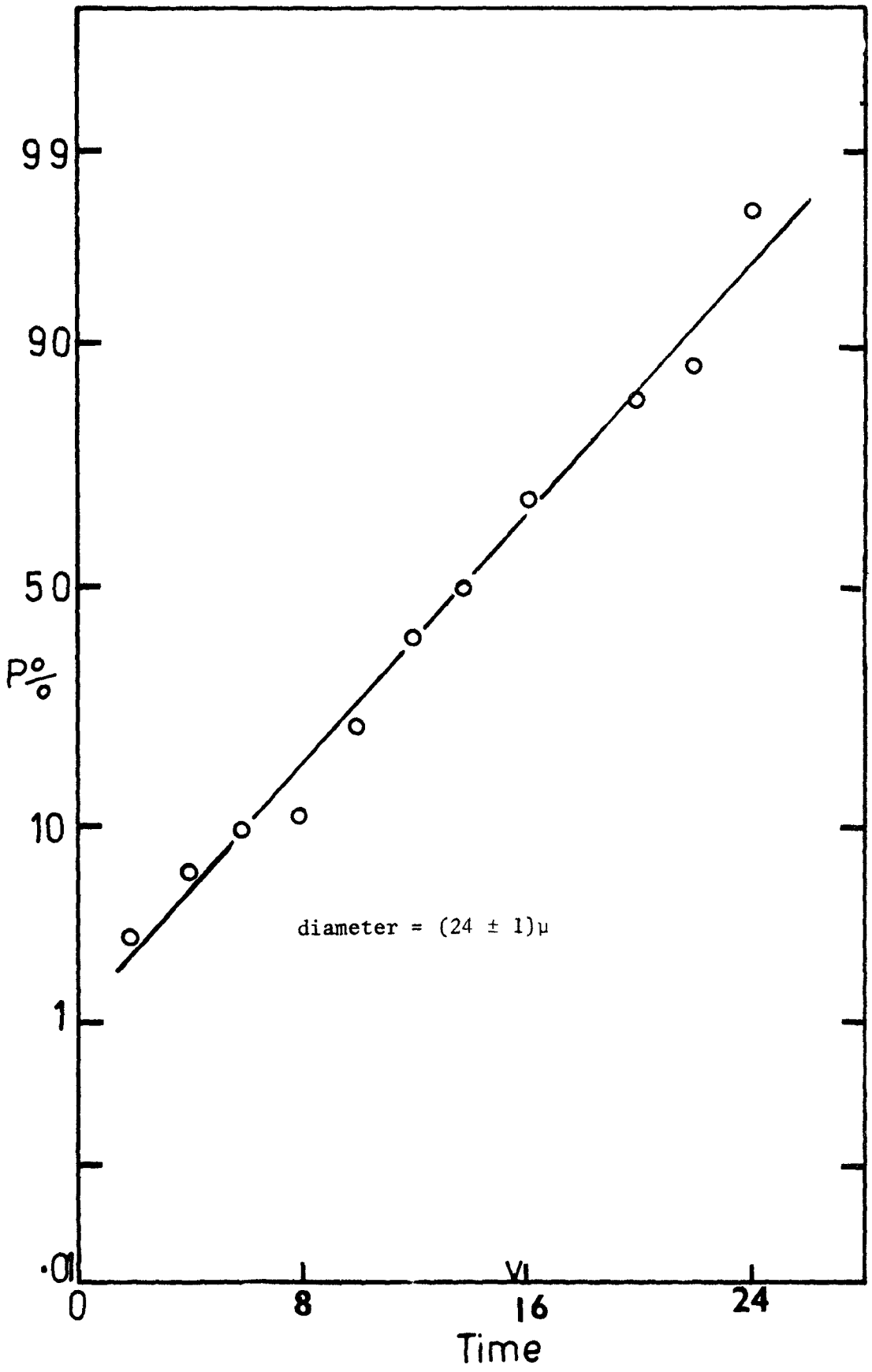

3d

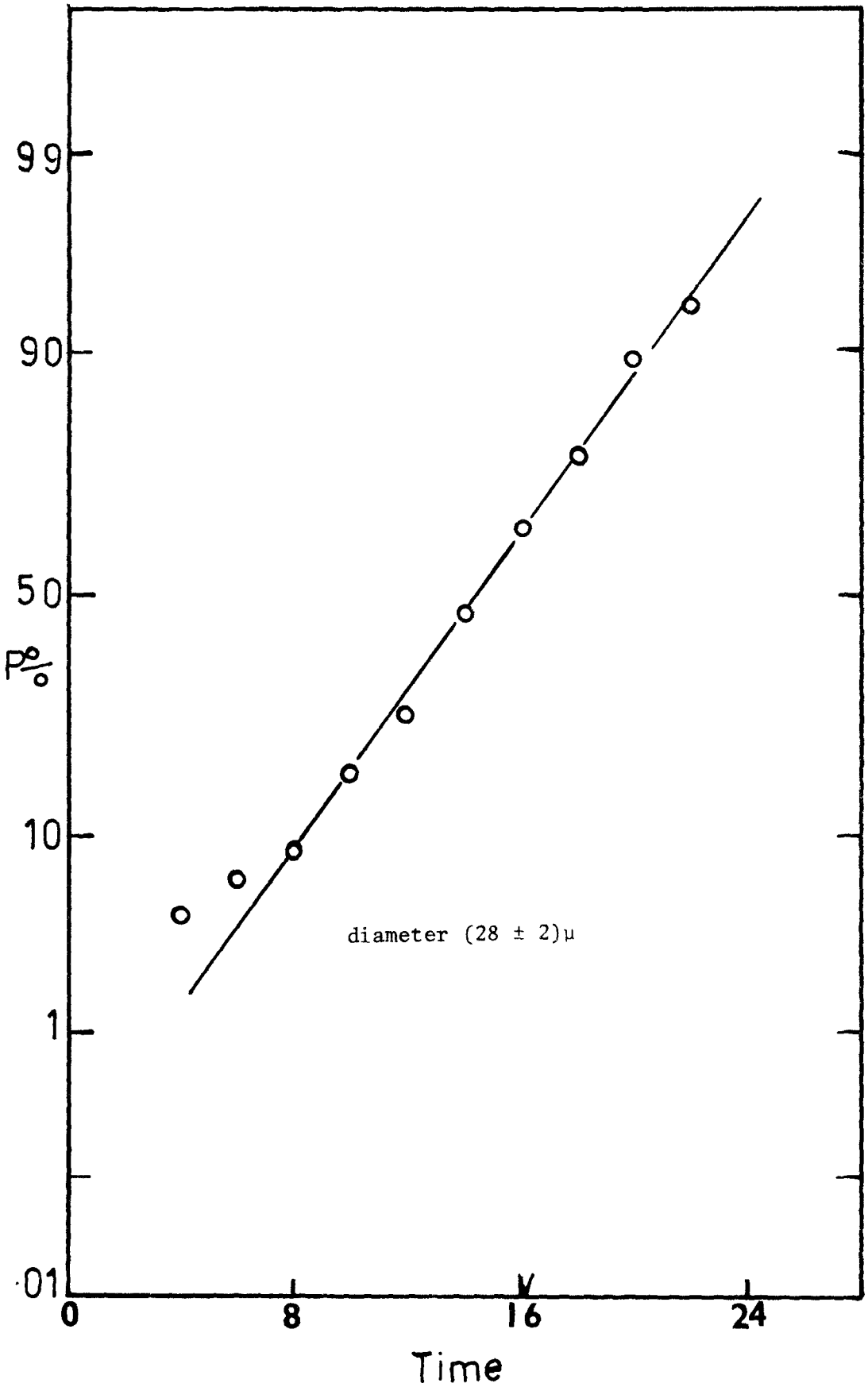

3e

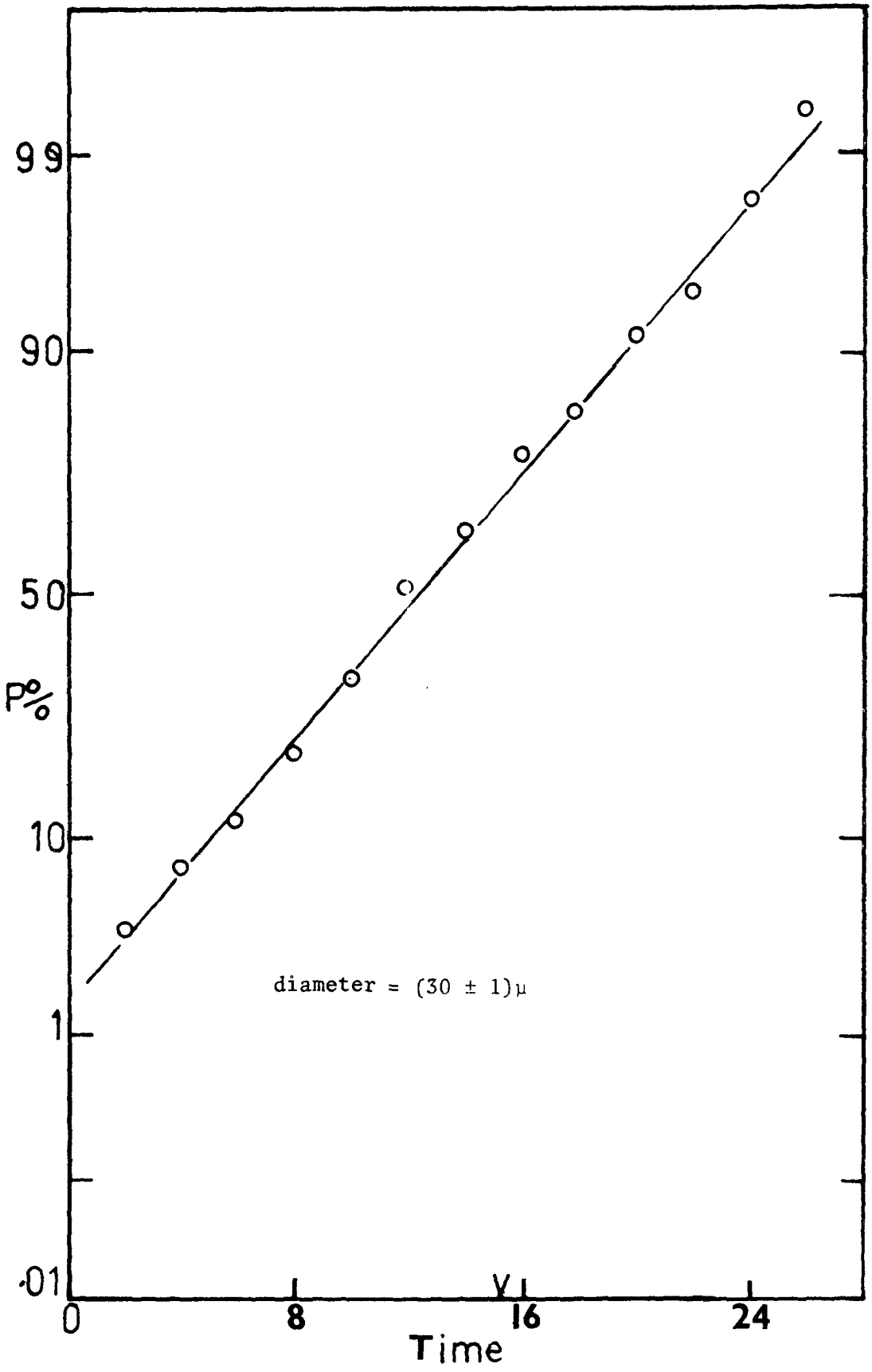
99
90
50
P%
10
1
·01
0
8
16
24
Time
diameter = (30 ± 1)μ

REFERENCES

1. D. B. Fahreinheit, Phil. Trans. Roy. Soc. 39, 78 (1724).
2. J. T. Lowitz, Crells Chemische Annalen 1, 3 (1735).
3. Lecoq de Boisbaudran, Compt. Rend. 63, 95 (1866).
4. G. W. Oswald, Z. Phys. Chem. 22, 289 (1897); 34, 493 (1900).
5. G. Tammann, Z. Physik. Chem. (Leipzig), 25, 441 (1898).
6. L. R. Ingersoll and E. C. Mendenhall, Phil. Mag. 15, 205 (1908).
7. B. Vonnegut, J. Colloid Sci. 3, 563 (1948).
8. C. Despretz, Compt. Rend. 4, 124 (1837).
9. L. Dufour, Phys. Z. 3, 195 (1902).
10. D. Turnbull, J. Appl. Phys. 20, 817 (1949).
11. M. Volmer and A. Weber, Z. Phys. Chem. (Leipzig), 119, 227 (1926).
12. L. Farkas and J. Szillard, Z. Phys. Chem. (Leipzig), A125, 236 (1927).
13. R. Becker and W. Doring, Ann. Physik, 24, 719 (1935).
14. M. Volmer, Z. Phys. Chem. 119, 277 (1926).
15. H. Daynes, Proc. Roy. Soc. (London), A97, 286 (1920).
16. W. G. Courtney, J. Chem. Phys. 36, 2009 (1962).
17. H. L. Frisch, J. Chem. Phys. 27, 90 (1957).
18. J. B. Zeldovitch, Acta Physicoch m. U.R.S.S. 18, 1 (1943).
19. D. Turnbull, Metal Tech. (June) 1948.
20. A. Kantrowitz, J. Chem. Phys. 17, 1097 (1951).
21. H. L. Frisch and C. C. Cartier, J. Chem. Phys. 54, 4326 (1971).
22. F. C. Goodrich, Proc. Roy. Soc. (London) A277, 180 (1964).
23. R. Defay and L. Dufour, "Thermodynamics of Clouds", Academic Press, New York, pp. 151 ff, 1963.
24. J. Frenkel, "Kinetic Theory of Liquids", Clarendon, Oxford, 1946.

25. W. H. Rodebush, Chem. Rev. 44, 269 (1949).

26. F. Kurt, Z. Phys. 131, 185 (1952).

27. J. Lothe and G. Pound, J. Chem. Phys. 36, 2080 (1962).

28. J. Lin, J. Chem. Phys. 48, 4129 (1968).

29. H. Reiss and J. Katz, J. Chem. Phys. 46, 2496 (1968).

30. F. Abraham and G. Pound, J. Chem. Phys. 48, 732 (1968).

31. A. G. Suhigin, Physics Letters, 26A, 5, 233 (1969).

32. S. Kondo, J. Chem. Phys. 48, 776 (1968).

33. R. C. Tolman, J. Chem. Phys. 17, 333 (1949).

34. J. G. Kirkwood and F. B. Buff, J. Chem. Phys. 17, 338 (1949).

35. Jean Yves Paslange, J. Crystal Growth, 6, 311 (1970).

36. G. C. Benson and R. Shuttleworth, J. Chem. Phys. 18, 130 (1951).

37. B. E. Sanquist and R. A. Oriani, J. Chem. Phys. 36, 2604 (1962).

38. F. L. Binsbergen, Kolloid-Zeitschrift and Zeitschrift fur Polymere, 2, 237 (1970).

39. A. G. Walton, J. Chem. Phys. 34 3162 (1963).

40. A. G. Walton and D. R. Whitman, J. Chem. Phys. 40, 2722 (1964).

41. B. V. Enüshun and J. Turkevich, J. Am. Chem. Soc. 82, 4502 (1960).

42. A. E. Nielson, Acta Chem. Scand. 15, 441 (1961).

43. A. G. Walton, Mikrochim. Acta, 422 (1963).

44. A. G. Walton, "Formation and Properties of Precipitates", Wiley and Sons, New York (1967).

45. A. E. Nielson, "Crystal Growth", Pergamon Press, Oxford, p. 419, 1967.

46. D. Mealor and A. Townshend, Talanta, 13, 1069 (1966).

47. A. G. Walton, "Nucleation", Dekker, New York, p. 206, 1969.

48. S. E. Kharin et al, Kolloidnyi Zhurnal, V. 31, N.I. 147 (1969).

49. J. A. Velazquez and O. E. Hileman, Can. J. Chem. 48, N. 18, 2896-2899 (1970).

50. J. A. Velazquez, Ph.D. Thesis, McMaster University 1970.

51. Jacobs and Tompkins in "Chemistry of the Solid State" by Garner, Butterworths Sci., London (1955), pp. 192.

52. H. E. Nielsen, Kristall und Technik, 4, 1, 17-38 (1969).

53. E. K. Bigg, Proc. Phys. Soc. 66B, 688 (1953).

54. A. E. Carte, Proc. Phys. Soc. 73, 324 (1959).

55. Dufour and Defay, reference 23, pp. 216-219.

56. J. A. Velazquez and O. E. Hileman, reference 49.

57. R. F. Strickland-Constable,"Kinetics and Mechanism of Crystallization", Academic Press, New York (1968), pp. 89.

58. A. G. Walton, see reference 47.

59. A. E. Nielsen, Proc. Intern. Symp. Nucleation Phenomena, Cleveland 17 (1965).

60. T. P. Melia, and W. P. Moffitt, Nature 201, 1024 (1964).

61. O. E. Hileman and J. A. Velazquez, Can. J. Chem. 48, 2896 (1970).

62. G. Clegg and T. P. Melia, Talanta 14, 989 (1967).

63. O. E. Hileman and J. A. Velazquez, Talanta 17, 623 (1970).

64. D. Mealor and A. Townshend, Talanta 13, 1069 (1966).

65. B. J. Mason and I. E. Kuhns, Proc. Roy. Soc. A., 302, 437-452 (1968).